Regional Alteration Mapping for Volcanic-hosted Massive Sulphide Exploration in the Pilbara, Australia

by

Oyungerel BAYANJARGAL

Thesis submitted to the
International Institute for Geo-information Science and Earth Observation
in partial fulfilment of the requirements for the degree of
Master of Science in Geo-information Science and Earth Observation for
Mineral Resource Exploration

Degree Assessment Board:

Dr. S.P. Vriend (Utrecht University; External examiner)
Prof. Dr. F.D. van der Meer (Chair)
Drs. F. van Ruitenbeek (1st supervisor, member)
Dr. E.J.M. Carranza (2nd supervisor, member)
Drs. J.B. de Smeth (Acting EREG Programme Director, member)

INTERNATIONAL INSTITUTE FOR GEO-INFORMATION SCIENCE AND EARTH OBSERVATION
ENSCHEDE, THE NETHERLANDS

Disclaimer

This document describes work undertaken as part of a programme of study at the International Institute for Geo-information Science and Earth Observation. All views and opinions expressed therein remain the sole responsibility of the author, and do not necessarily represent those of the institute.

Abstract

The main purpose of this thesis is to use modern techniques such as remote sensing (RS) and geographic information system (GIS) to detect hydrothermal alteration systems related with volcanic-hosted massive sulphide (VhMS) deposits in the East Pilbara Granite-Greenstone Terrain (EPGGT) of Western Australia.

Remote detection of the hydrothermal alteration systems was done using Landsat TM imagery and K-channel of gamma-ray spectrometry. A method was developed to detect hydrothermal alteration systems in Kangaroo Caves using normalised potassium and Landsat ratio image based on the previous studies. The normalisation method was later applied to other parts of the EPGGT, which have similar geological setting as the Kangaroo Caves. Each of the areas consists of a volcano-sedimentary sequence and is underlain stratigraphically by a felsic intrusion.

An interpretive map of hydrothermal alteration systems related with VhMS deposit in EPGGT was produced during this study and validated using known mineral deposits. In this map, potential hydrothermal discharge zones are indicated and then weighted based on interpretations of alteration rates.

Potential VhMS deposits are located in areas where crosscutting discharge related alteration intersects the paleo-seafloor at the top of a bi-modal volcanic sequence. Therefore, detection of the top of a volcanic sequence that is felsic and the position of the paleo-seafloor has a high priority in detection of potentially mineralised areas.

Keywords: Hydrothermal alteration systems, VhMS deposits, Kangaroo Caves, EPGGT, normalisation, potential discharge zone

Acknowledgement

I would like to express my gratefulness to the Dutch government who was in charge of the financial support for my study at ITC and also my deep gratitude to Prof. Dr. A.Bayasgalan, Director of School of Geology, Mongolian University of Science and Technology.

My special thanks to my colleague B.Enkhtuvshin, who recommended me to undergo MSc programme in mineral exploration field and his kind advise. I am also very thankful to Kelly Cluer for his support and to my colleagues from Cameco Gold Mongolia Inc. I appreciate to G.Ukhnaa and Altanlish who had given me significant recommendations for applying to the ITC.

Special acknowledgement is given to my supervisors of the thesis, Drs. F. van. Ruitenbeek and Dr. E.J.M. Carranza, for their support on my research work and their guidance. I would like to thank to Drs. J.B. de Smeth for his support, kind courtesy and his guidance for remarkable fieldwork in Spain and Portugal. My deep gratitude is to Dr. Kim A.A. Hein for her nice discussions, valuable advices and her amity.

I thank widely to my friends Ronald, Tumee, Paul, Tumruu, Tsomo, Todoo, Carlos, Ulan, Marleen, Esther, Kim, Rafael, Segundo, Aiman, Analia and all my country fellows for sharing memorable moments with me during this period in ITC. I would like to thank to Pablo, his family, and to all my classmates in the Mineral Resource Exploration specialisation and to all EREG2002 M.Sc. students. And also thanks to members of volleyball team of ITC for the most enjoyable time.

Finally I would like to thank to my parents, sisters, brothers and my boyfriend who have given me the strength to go on.

Thanks to everyone who helped me and I wish all of you a wonderful happy days.

Oyungerel Bayanjargal
2004, Enschede
The Netherlands

Dedicated to my father
Аавдаа зориулав ...

Contents

List of figures

List of tables

List of Abbreviations

VhMS	Volcanic-hosted Massive Sulphide
RS	Remote Sensing
GIS	Geographic Information System
EPGGT	East Pilbara Granite-Greenstone Terrain
WPGGT	West Pilbara Granite-Greenstone Terrain
MB	Mallina Basin
KT	Kuranna Terrain
MCB	Mosquito Creek Basin
AGSO	Australian Geological Survey Organisation
GSWA	Geological Survey of Western Australia
TM	Thematic Mapper
SS	Sulphur Springs
KC	Kangaroo Caves
BK	Breakers
MW	Man of War
RM	Roadmaster
SG	Sharks Gully 2

CHAPTER 1: Introduction

1.1. Preface

The topic of this thesis is detection of hydrothermal alteration systems related to Volcanic-hosted Massive Sulphide (VhMS) deposits of 3.72-2.85 Ga East Pilbara Granite-Greenstone Terrain (EPGGT) within the Pilbara Craton in Australia, which is host to the oldest VhMS mineralisation in the world.

Exploration geologists are engaged not only in the search for new mineral deposits, but also in the extension and re-assessment of existing ones [1]. To succeed in this task, the exploration geologist is required to be up to date with the latest developments in the evolution of concepts, ideas and techniques in the earth sciences. Therefore, the main purpose of this thesis is aimed to use modern techniques such as remote sensing (RS) and geographic information system (GIS) to detect hydrothermal alteration systems. Hydrothermal activity, in its broadest sense, is responsible for a very wide range and variety of metallic ore deposits. Detection of hydrothermal system is major advantage of the early exploration stages to find ore deposits.

1.2. Study area

The research area is located in the North Pilbara Terrain of the Pilbara Craton, Western Australia (Figure 1.1). The North Pilbara Terrain is a good study area where applications for the development of new methods for RS and GIS based detection of hydrothermal alteration mapping can be demonstrated to be useful. This terrain has good exposures of well-studied hydrothermal alterations related to mineralisation. But effective studies of technique and application are still lacking in most of the area except Kangaroo Caves, which is a well-studied hydrothermal alteration system in EPGGT.

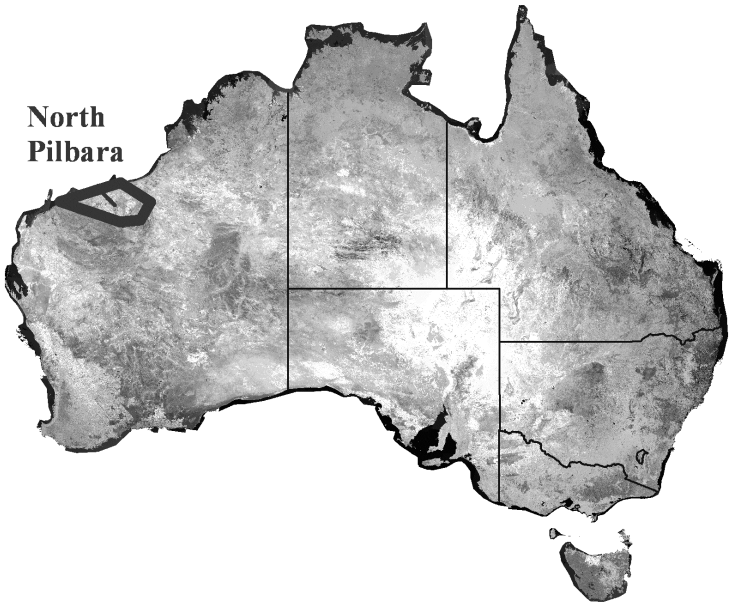

Figure 1.1: Location map (source [2]).

1.3. Problem definition

The North Pilbara terrain constitutes one of the most abundant and interesting VhMS regions in Australia. AGSO (Australian Geological Survey Organisation) and GSWA (Geological Survey of Western Australia) studied the geology and applications of RS techniques to this region under the North Pilbara Project (1995-2000) and produced a complete dataset for the area. During these years, the project acquired gamma-ray spectrometric data over the Panorama district and studied remote alteration mapping by gamma-ray spectrometry in the district. Much of previous works on alteration systems associated with VhMS mineralisation are confined to some place such as Panorama district [3, 4] and Kangaroo Caves deposit [5].

Several geologists have also studied to map alterations systems [3] by traditional methods, but till now such studies could not map large areas at short periods. Therefore there is a necessity to demonstrate that mapping of regional-scale hydrothermal alteration systems associated with VhMS mineralisation by using remotely sensed data based on detailed studies of deposits, such as Kangaroo Caves deposit.

Remote sensing images are used in mineral exploration to detect indications of mineral deposits, specifically by recognition of hydrothermally-altered rocks that have specific spectral signatures. Processed Landsat TM images can be used to identify groups of but not individual hydrothermal alteration minerals over large areas. Such recognition of groups of hydrothermally-altered rocks from Landsat TM images can be a valuable regional-scale exploration tool in delineating potential zones for follow-up work. It is useful to distinguish between hydrothermally-altered rocks that are more associated to the deposit type. This requires RS techniques that can detect specific types of hydrothermal alteration systems.

To enhance the alteration information, geologists usually delineate altered rocks by visual interpretation instead of automatic technique. Such a case has a low accuracy and low working efficiency, and therefore cannot meet the needs of geological exploration.

Therefore, it is interesting to tackle the problem of how to use Landsat TM data for enhancement and automatic delineation of altered rocks.

The quality of gamma-ray spectrometric surveys has improved in recent times so that absolute concentrations of potassium, uranium, and thorium in altered and fresh rocks can be well estimated. Hence, airborne gamma-ray spectrometry can effectively map specific hydrothermal alteration zones, particularly in well-exposed areas. Mass changes and in particular K-depletion in hydrothermal alteration zones associated with VhMS deposits yield information on hydrothermal alteration and fluid-rock interactions, and provide another criterion for selecting exploration targets for locating sulphide mineralisation [4, 6, 7].

It is important but not simple to find (ancient) hydrothermal vents where VhMS deposits might occur, but it might be useful to define recharge and discharge zones that can probably indicate favourable sites for VhMS deposits. Landsat TM images can indicate presence of white micas (hydrothermally formed), which are useful markers of certain positions in a hydrothermal alteration system. Gamma-ray spectrometry indicates K concentration and K depletion, which can improve the detection of hydrothermal vent sites [5]. Together they can provide indications of most hydrothermal alteration facies in hydrothermal alteration system recharge zones (i.e., increase in white mica and K enrichment in basalts) and discharge zones (i.e., K depletion and absence of white micas). The two data types provide complementary information that can increase the possible detection of a paleo-hydrothermal system and associated VhMS deposit.

1.4. Main research question

Can we detect regional scale hydrothermal alterations associated with VhMS deposits by mapping variations in K concentration using regional airborne gamma-ray spectrometry and the distribution of alteration minerals from Landsat TM, in the East Pilbara Granite-Greenstone Terrain?

1.5. Research objectives

The major objective of this study is to apply RS and GIS-based techniques for the interpretation of specific hydrothermal alteration zones using various datasets in the North Pilbara Terrain. Within this major objective, the research specifically aims to:

- To model the K-concentration and white mica abundance in the Kangaroo Caves hydrothermal alteration system.
- To determine whether and how the Kangaroo Caves alteration system can be detected from airborne gamma-ray data and processed Landsat TM images.
- To map the K distribution (enrichment and depletion) in volcanic rocks in the study area.
- To map the abundance of white micas and other phyllosilicates in volcanic rocks in the study area
- To interpret these in terms of paleo recharge and discharge zones.
- To create a favourability map for VhMS deposits.
- To validate the favourability map using known mineralisations.

1.6. Structure of the Thesis

The thesis has seven chapters. Chapter 1 deals with the main problems behind this thesis, its research question and objectives. Chapter 2 describes the regional geology, mineralisation and hydrothermal alteration system within the Archaean greenstone belts in the North Pilbara Terrain from the literatures related to the research. Chapter 3 describes datasets used and depicts methodologies considered for this research. Chapter 4 and 5 describe methods for remote detect Kangaroo Caves alteration system and hydrothermal alteration system related to VhMS deposits within the EPGGT. Chapter 6 deals with discussion of the results and Chapter 7 makes conclusion and recommendation based on data and interpretations presented in each of the chapters.

CHAPTER 2: Background

2.1. Geology

2.1.1. Pilbara Craton

The Pilbara Craton is composed of (inset of Figure 2.1) two principal components: (a) a Palaeo- to Neo-Archaean (3.72-2.85 Ga) basement of granitoids and greenstone belts, which are exposed in several inliers, including a large area in the north of the craton known as the North Pilbara Terrain, and (b) Volcano-sedimentary rocks of the Neo-Archaean (2.77-2.40 Ga) Mount Bruce Supergroup which where deposited in the Hamersley basin. The Mount Bruce Supergroup unconformably overlies the older granitoid-greenstone basement [8].

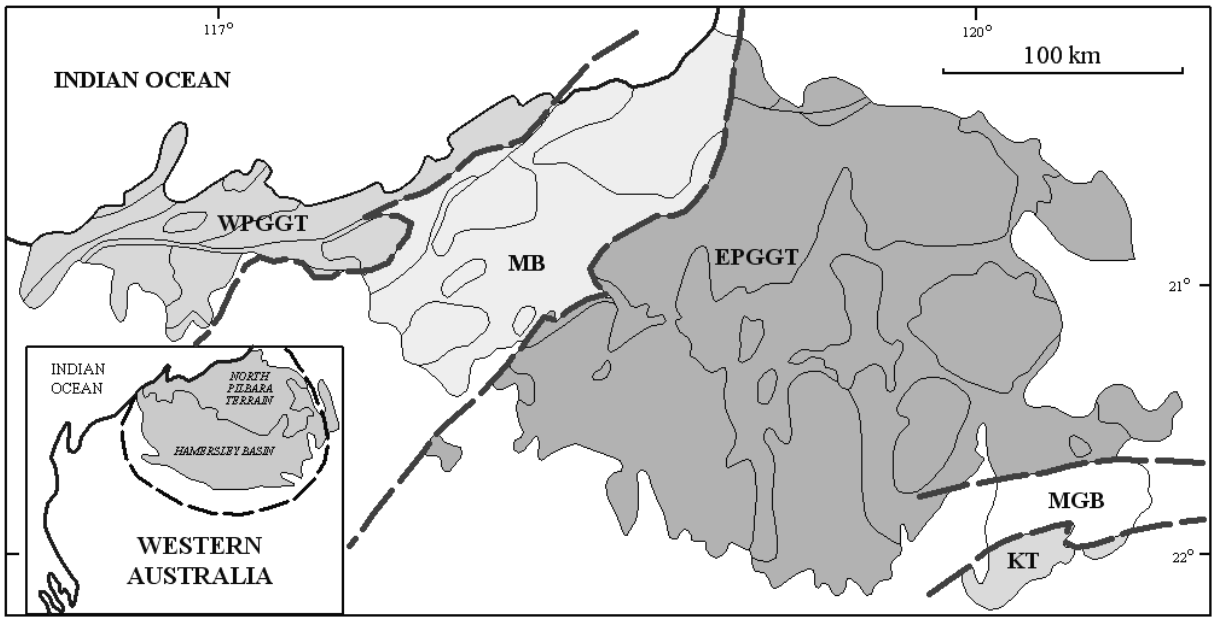

Figure 2.1: Five main lithotectonic elements of North Pilbara Terrain: West Pilbara Granite-Greenstone Terrain (WPGGT); Mallina Basin (MB); East Pilbara Granite-Greenstone Terrain (EPGGT); Mosquito Creek Basin (MGB); and Kuranna Terrain (KT). Inset shows position of Pilbara Craton in Western Australia (heavy dashed line). Source [3, 8, 9]

2.1.2. North Pilbara Terrain

The North Pilbara Terrain is composed of three separate granite-greenstone terrains with distinct stratigraphy and unique geochronological and structural histories, separated by sedimentary basins formed in active tectonic zones. Therefore, the North Pilbara Terrain is subdivided into five lithotectonic domains (Figure 2.1): (1) The East Pilbara Granite-Greenstone Terrain (EPGGT) that formed between 3.72-2.85 Ga; (2) The ca. 3.27-2.92 Ga West Pilbara Granite-Greenstone Terrain (WPGGT); (3) The ca. 3.01-2.94 Ga Mallina Basin (MB) which is composed of metamorphosed volcanic and sedimentary rocks, and associated granitoid, The Mallina Basin was deformed at 2.95-2.93 Ga. (4) The Kuranna Terrain (KT) in the south-east of the craton, which is composed largely of granitoid rocks dated at ca. 3.3-3.2 Ga and separated from the East Pilbara Granite-Greenstone Terrain by the Mosquito Creek Basin (MCB); (5) The Mosquito Creek Basin of undated turbiditic clastic rocks deformed into a fold and trust belt at ca. 2.9 Ga [8].

2.1.3. East Pilbara Granite-Greenstone Terrain (EPGGT)

The EPGGT represents the ancient cratonic nucleus of the North Pilbara Terrain, with a geologic history spanning 870 m.y., from 3.72 to 2.85 Ga. It is composed of some of the best-presented, oldest life on Earth, is host to some of the oldest mineral deposits on Earth, and represents the type example of a dome and basin map pattern that is unique to Archaean terrains. The EPGGT is also well known because of the ongoing controversy regarding the tectonic evolution that gave rise to this map pattern [8].

The EPGGT is characterized by large (35-120 km. diameter in map view), ovoid, domical granitoid complexes (Figure 2.2) and flanking, curviplanar, generally synclinal tracks of generally steeply dipping volcano-sedimentary rocks collectively referred to as greenstones (Figure 2.3). Greenstone belts are defined as relatively well preserved tracts of generally coherent greenstone stratigraphy bounded by faults, intrusive and/or sheared intrusive contacts with granitoid complexes, unconformably overlying supracrustal rocks of the Fortescue Group and younger cover. Greenstone complexes are areas of high structural complexity in which a coherent stratigraphy is generally lacking and faulting and/or shearing is common [8].

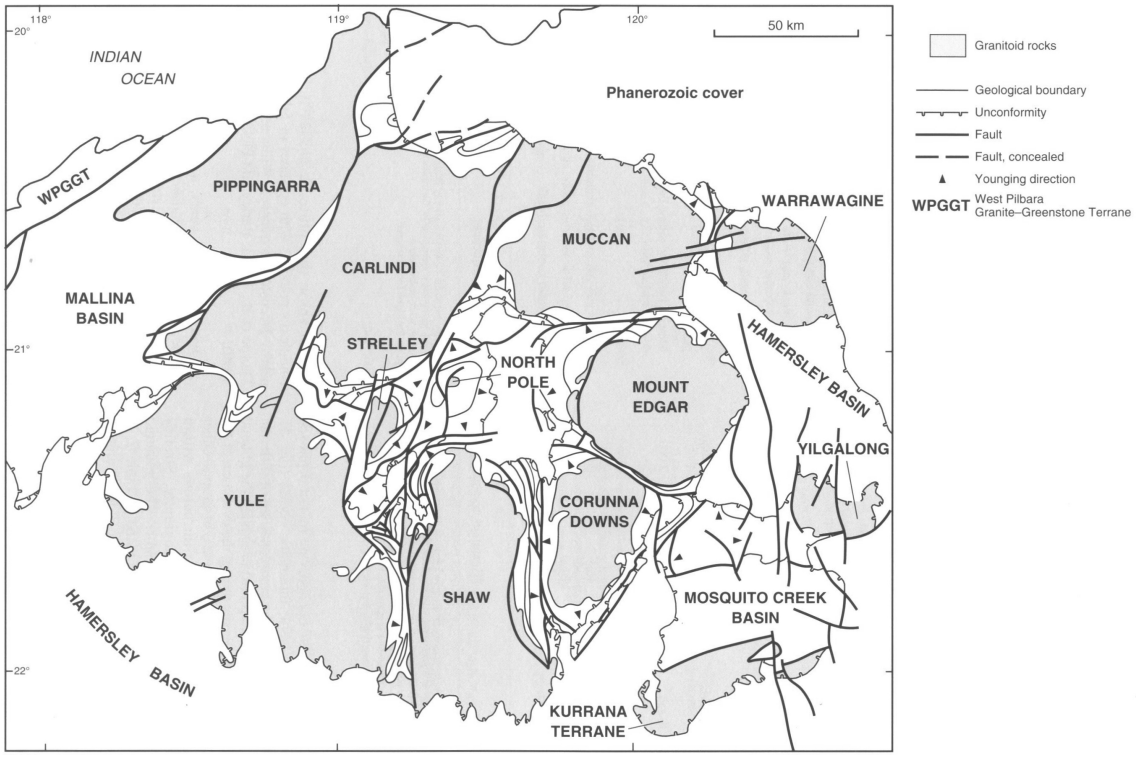

Figure 2.2: Distribution of Archaean granitoid complexes and plutons (in grey) in the EPGGT. Source [8, 9]

Lithostratigraphy

The Pilbara Supergroup of the EPGGT is formally divided into five volcano-sedimentary groups and two formations that include, from base to top: the ca. 3.51 to 3.50 Ga Coonterunah Group; the ca. 3.49 to 3.31 Ma Warrawoona Group; the ca. 3.26 to 3.24 Ga Sulphur Springs Group; the undated Gorge Creek Group deposited between 3.24 Ma and 2.94 Ga; the ca. 2.94 Ga De Grey Group. The ca. 3.31 Ga Budjan Greek Formation lies unconformably on the Wyman Formation in the Kelly greenstone belt and is unconformably overlain by the Gorge Creek Group. The undated Golden Cockatoo Formation in the Yule Granitoid Complex is bounded by faults and intrusive contacts with granitoid rocks but is probably related to deposition of the adjacent Sulphur Springs Group [8].

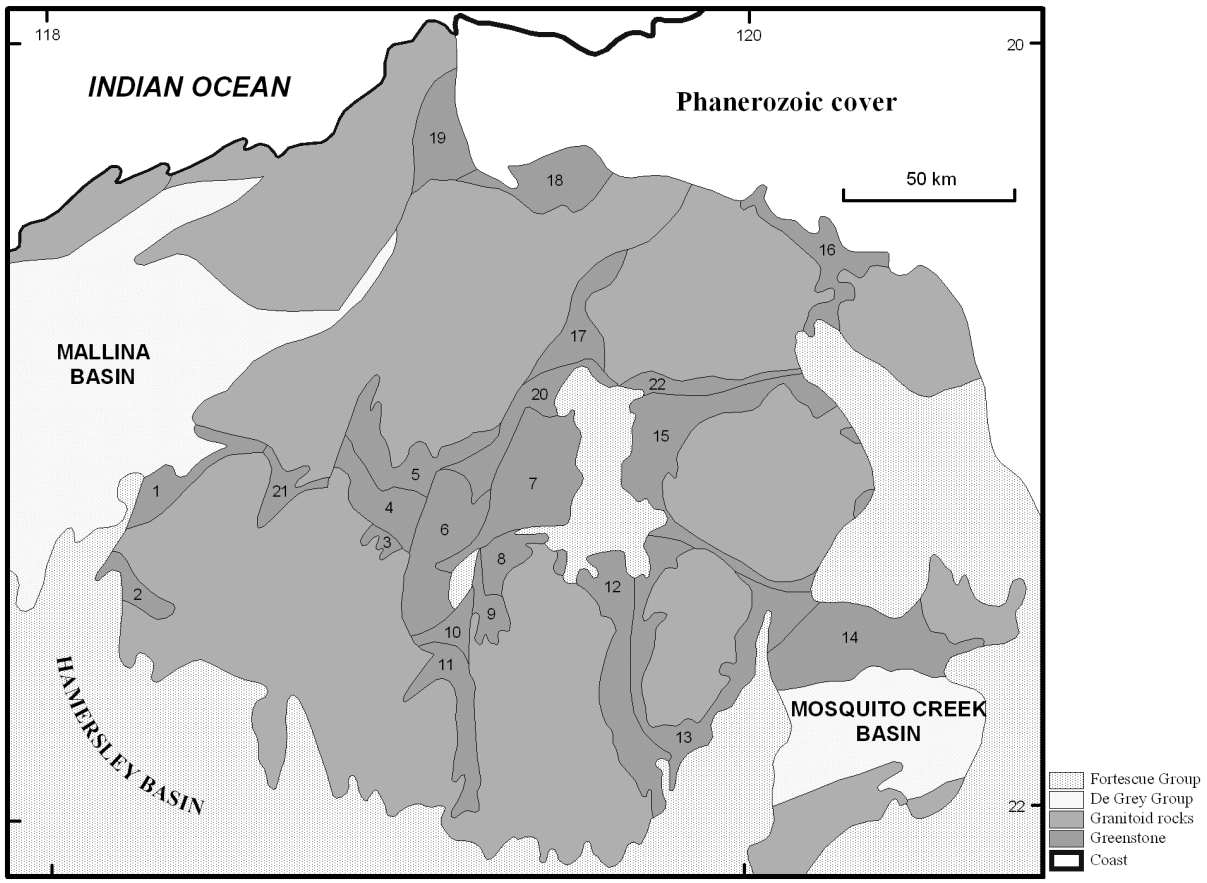

1. Pilbara greenstone belt	9. North Shaw greenstone belt	17. Warralong greenstone belt
2. Cheeara greenstone belt	10. Tambina complex	18. Goldsworthy greenstone belt
3. Abydos greenstone belt	11. Western Shaw greenstone belt	19. Ord Range greenstone belt
4. Pincunah greenstone belt	12. Coongan greenstone belt	20. Lalla Rookh greenstone belt
5. East Strelley greenstone belt	13. Kelly greenstone belt	21. Wodgina greenstone belt
6. Soanesville greenstone belt	14. McPhee-Elsie greenstone belt	22. Doolena Gap greenstone belt
7. Panorama greenstone belt	15. Marble Bar greenstone belt	
8. North Shaw greenstone belt	16. Shay Gap greenstone belt	

Figure 2.3: Distribution of Archaean greenstone belts in the EPGGT. Source [8, 9]

Greenstone sequences

The greenstones are assigned to the Pilbara Supergroup and include metamorphosed mafic to ultramafic volcanic rocks, felsic to intermediate volcanic rocks, clastic sedimentary rocks, chert, banded iron-formation, and sills of mafic to ultramafic intrusive rocks. The distribution of greenstone sequences and the names of the greenstone belts are shown on Figure 2.3 [9].

Granitoid complexes

The granitoid complexes in the EPGGT are large, domal, composite bodies that consist of syntectonic granitoid intrusions, gneissic granitoid, and migmatite; some complexes contain enclaves of metamorphosed greenstones of layered mafic-ultramafic bodies (Figure 2.2). The various components of the complexes are of different ages and they have been interpreted to explain the gradual development of the Pilbara Craton Other granitoid bodies occur as discrete intrusions within greenstone belts: North Pole Monzogranite, Strelley Granite, and Keep It Dark Monzogranite [9].

Structural geology

Two types of regional structures occur in the EPGGT; a dome and basin pattern comprising granitoid-cored domes and a 5 to 15 km-wide, north-south-striking, curvilinear zone of complex folds and faults referred to as the Lalla Rookh-Western Shaw structural corridor, which transects the EPGGT (Figure 2.4) [8].

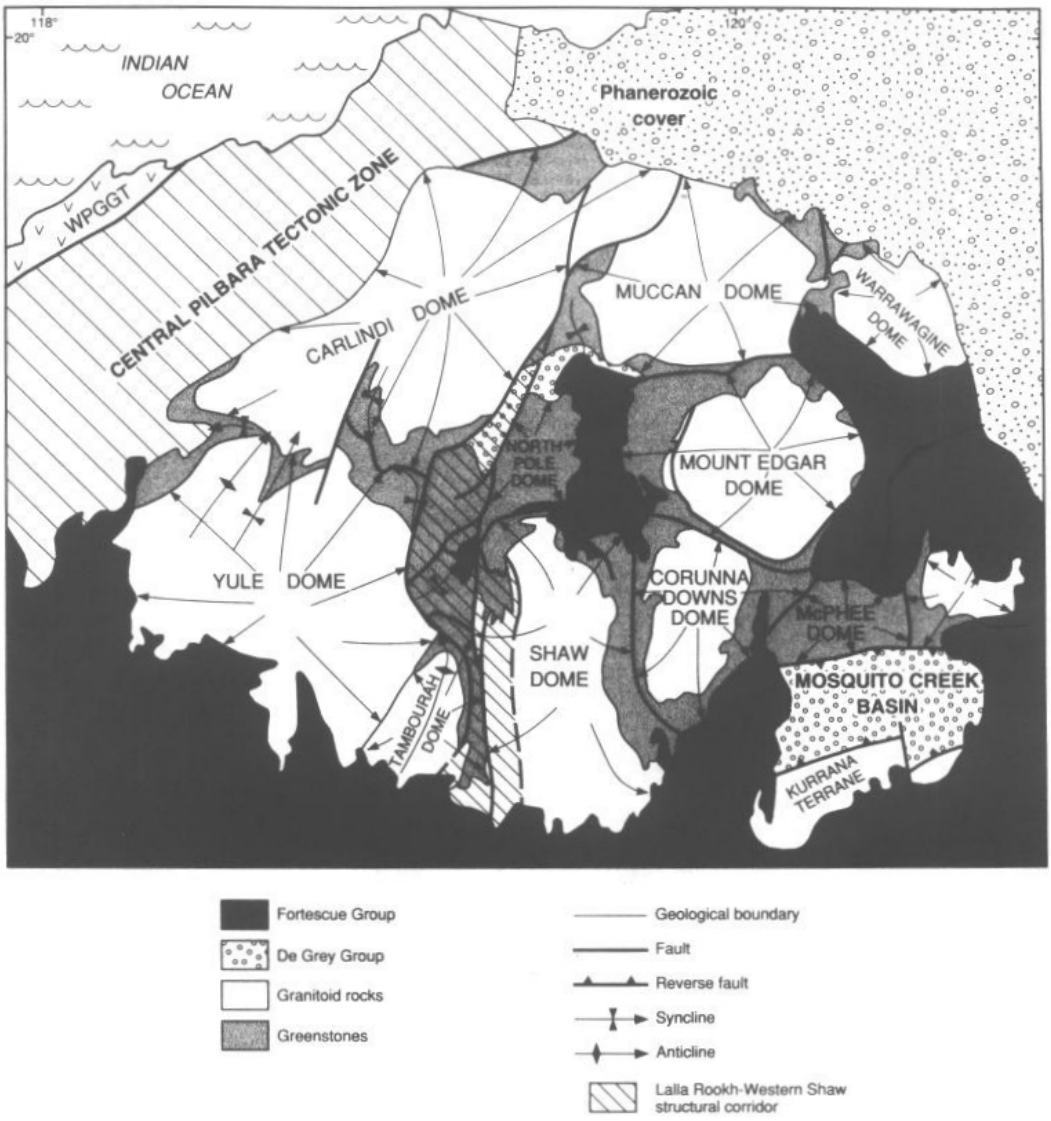

Figure 2.4: Schematic map of large-scale structures of the EPGGT. Bold names refer to granitoid-cored domes that formed throughout the development of the terrane. Source [8]

Structural domes include a core of granitoid rocks and a rind of greenstones that are attached to the granitoid rocks by intrusive or sheared intrusive contacts. Ring faults in the axes of intervening greenstone synclines separate the structural domes (Figure 2.4). Granitoid complexes typically contain areas of migmatitic gneiss with evidence of multiphase deformation, but their margins commonly have a single foliation that dips steeply and is parallel to, and passes across, contacts with greenstones. Adjacent greenstones have shallow (e.g., Panorama and northwestern Marble Bar greenstone belts) to steep (e.g., East Strelley and Coongan greenstone belts) dips and generally display a single foliation. Farther away from granitoid contacts, greenstones commonly have

subvertical dips and display a single foliation, although bedding-parallel high-strain zones may contain multiple, overprinting foliations [8].

Some structures in the following section have been grouped together in broad events.

D_1 (ca. 3490-3410 Ma): D1 structures include local tilting of the Coonterunah Group and Talga Subgroup away from the cores of granitoid complexes prior to deposition of the Panorama Formation and Apex Basalt respectively. They also include synvolcanic, listric, normal growth faults in the Dresser Formation, the Duffer Formation, and the Panorama Formation.

Complex folds, overturned bedding, and anomalously high-pressure metamorphic mineral assemblages occur in the northwest Shaw area, which were interpreted to represent D_1 structures resulting from Alpine-style thrusting that preceded doming of the Shaw Granitoid Complex. Gneissic fabrics and rootless isoclinal folds of leucosome veins in >3.45 Ga protoliths of the Shaw Granitoid Complex are also interpreted as D_1 structures, as they are cut by weakly foliated granitoid rocks dated at ca. 3.43 Ga [8].

D_2 (ca. 3315 Ma): These structures were generated between deposition of the Wyman and Budjan Creek Formations during intrusion of granitoid rocks at ca. 3315 Ma in the Corunna Downs and Mount Edgar Granitoid Complexes.

D_3 (ca. 3240 Ma): Intrusion of the Strelley Granite resulted in a suite of synvolcanic growth faults in the Kangaroo Caves Formation during hydrothermal circulation and massive sulphide deposition at 3240 Ma.

Sulphur Springs Group volcanism was accompanied by intrusion of granitoid rocks in the northeastern part of the Yule Granitoid Complex, including the Tambourah dome. Deposition of the Gorge Creek Group occurred during the late stages of D_3 doming in the Pincunah greenstone belt, where the basin was affected by syndepositional horst and graben faults.

D_4 (ca. 2940 Ma): Deformation affected much of the North Pilbara terrain at ca. 2940 Ma and resulted in the formation of the northerly striking Lalla Rookh-Western Shaw structural corridor in the EPGGT and deposition of the De Grey Group (Figure 2.4).

Two strands of sinistral shear formed along the western margin of the Shaw Granitoid Complex at this time and are known collectively as the Mulgandinnah shear zone.

D_4 deformation also caused amplification of the Tambourah dome, low-grade metamorphism of adjacent greenstones, and development of a north-northeast-striking foliation defined by oblate quartz grains in granitoid rocks of the Yule and Shaw Granitoid Complexes.

D_5 (ca. 2890 Ma): Sinistral shearing on north-northeast-striking zones affected the northwestern part of the EPGGT at ca. 2890 Ma and was accompanied by epigenetic gold mineralisation in the Mount York and Lynas districts. It is not known to what tectonic events this shearing relates, but it is the last deformation to affect the basement rocks prior to cratonization marked by the emplacement of post-tectonic granitoids at 2850 Ma.

D_6 (ca. 2760 Ma): The unconformably overlying, predominantly basaltic volcanic rocks of the Fortescue Group record a late component of granitoid doming. This is evidenced by the fact that outliers of the Fortescue Group in the EPGGT are preserved only in synclines that are developed over older synclines in greenstones between domical granitoid rocks.

Metamorphism

Metamorphic temperatures in greenstones decrease away from granitoid complexes from lower amphibolite facies, to greenschist and prehnite-pumpellyite facies, to very low temperature metamorphism of the De Grey and Fortescue Groups. Two-pyroxene granulite remnants have been recorded in amphibolite in the Shaw and Yule Granitoid Complexes. The highest pressure estimates of ca. 6 kbars have been obtained from kyanite-bearing felsic schists in the northwestern Shaw area and southern Marble Bar greenstone belt.

Amphibolite-facies metamorphism of the Western Shaw greenstone belt was dated at ca. 3234 Ma and greenschist-facies metamorphism at ca. 2950 Ma-the two dates ascribed to D3 doming and D4 transpression, respectively [8].

2.2. Hydrothermal Alteration Systems and VHMS deposits

2.2.1. Panorama district

The ca. 3.24 Ga Panorama VhMS district, which is located in the Pilbara Craton of Western Australia (Figure 2.5), is hosted by well exposed hydrothermal alteration system in a volcanic succession, including a subvolcanic intrusion, in an area of low metamorphic grade and very low strains that is virtually unweathered. There is remarkable preservation of original structures and textures, which show the deposits to be analogues to those forming in modern oceanic setting [3, 4]. The mineralised sequence has been gently folded, such that a complete section from the underlying subvolcanic intrusion, through the volcanic pile which hosts the VhMS deposits, to the overlying sedimentary succession, is exposed in an area of exceptional outcrop.

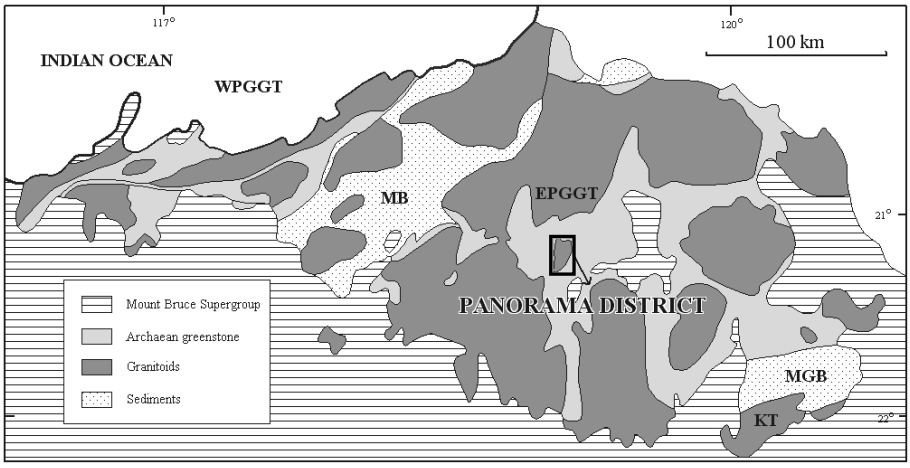

Figure 2.5: Location of the Panorama VhMS district. Source [3, 8]

Four major alteration facies are recognized in the volcanic and intrusive rocks in the Panorama district, with a series of subdivisions in each facies. Alteration facies are not lithology specific, but are developed in all lithologies from andesite-basalt, through rhyolite, to granite. The four alteration facies are the following [3]:

1. ***Background alteration***, which is akin to spilitic alteration in basalt, and keratophyric alteration in felsic rocks, is typified by an albite and/or K feldspar-chlorite-calcite and/or ankerite-quartz-pyrite+-leucoxene+-magnetite+-sericite assemblage.
2. ***Feldspar-sericite-quartz alteration*** is commonly characterized by a K feldspar and/or albite-sericite-quartz-ankerite-leucoxene+-pyrite assemblage. In rocks transitional to background alteration, minor chlorite is present.
3. ***Sericite-quartz alteration*** is completely feldspar-destructive and is typically a quartz-sericite-leucoxene+-ankerite+-pyrite assemblage.
4. ***Feldspar-destructive chlorite-quartz alteration*** is defined by a quartz-chlorite-sericite+-leucoxene+-hematite assemblage, in which pyrite+-base metal sulphides and ankerite-siderite are only developed immediately beneath zones of base metal mineralisation.

2.2.2. Kangaroo Caves

One of the VhMS deposits in the Panorama district is Kangaroo Caves. In the Kangaroo Caves, alteration zones developed by hydrothermal fluids. The alteration zones developed in volcanic wall rock, underlying Kangaroo Caves mineralisation, have a strong spatial association with feldspar-destructive alteration centres within the Strelley Granite.

The geochemistry and mineralogy of volcanic wall rock, in particular the distribution of K and white micas in the hydrothermal system that is associated with the Kangaroo Caves deposit has been well studied [5]. Based on their variation six hydrothermal alteration facies (or groups) have been determined in the volcanic rock underlying this deposit. Their composition is shown in box and whisker plots in Figure 2.6, together with the temperature of hydrothermal alteration, obtained from oxygen isotope data [5].

Group 1: Strongly silicified and occur within 400 m of the top of the volcanic sequence in felsic rocks. Their main characteristic is enrichment in Si; their Fe and Mg content are not very high and they contain some Na, Ca, and K. Both white mica and chlorite is abundant though white mica dominates. The absorption wavelength is short, which indicates Al-rich white mica. Microprobe analyses of white micas indicate K-deficiency. The temperature of alteration of this group is relatively low (175ºC). This group of rocks is interpreted as hydrothermally altered by relatively low temperature silica rich fluids where Al-rich white micas were formed.

Group 2: Rich in K and poor in Fe and Mg and Na, which is expressed by a high Al. This group occurs in felsic rocks in the upper part of the volcanic sequence. White mica, which is Al-poor, is abundant and chlorite is absent in all samples. Temperature of alteration is 225ºC on average. The type of alteration that has affected this group of felsic rocks is interpreted as potassic alteration due to medium temperature fluids with relatively high K activities, low K and Mg and not very high water/rock ratios, where Al poor white mica is formed and ferro-magnesian minerals are absent.

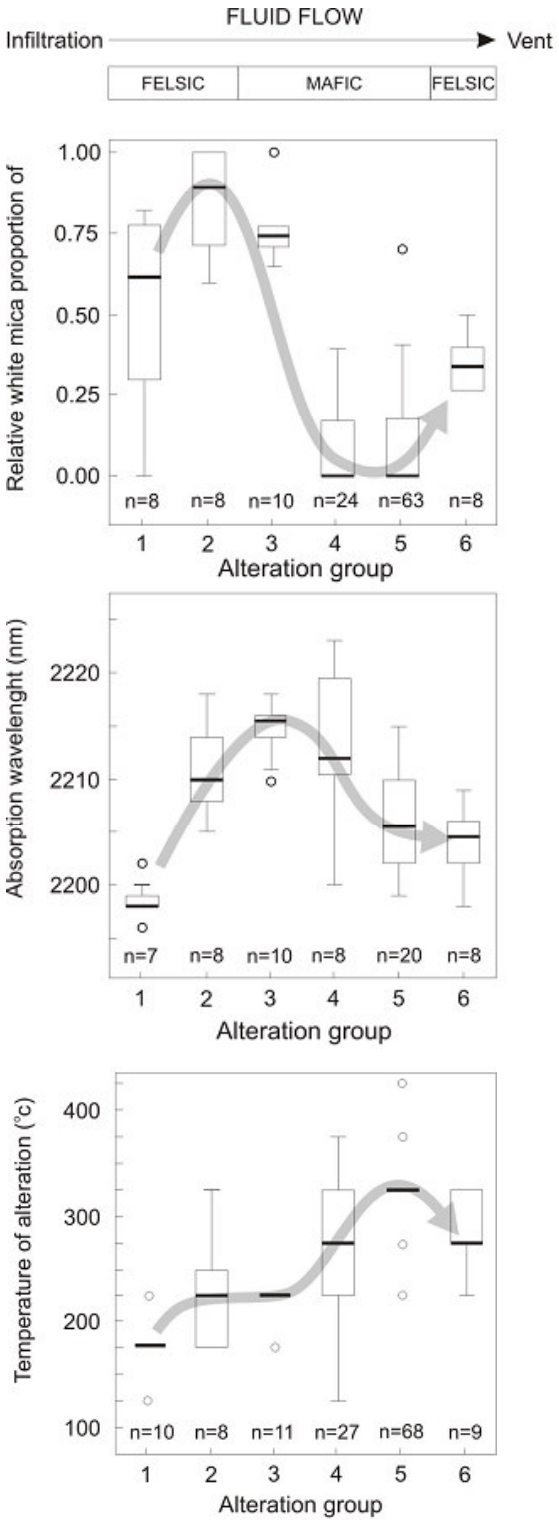

Figure 2.6: White mica proportion, absorption wavelength and temperature of hydrothermal alteration of 6 alteration facies developed in volcanic rock [5]

Group 3: Rich in K and poor in Fe and Mg. The alteration style is similar to the group 2. However the lithology is mafic and these units occur stratigraphically below the K altered felsic rocks.

Group 4: Less than 80% of Al and somewhat enriched in Fe and Mg and depleted in K. Some Na and Ca are present. All samples of this group are derived from mafic volcanic rocks and contain abundant chlorite while only about 30% contains minor white mica, which the composition is variable though generally Al-poor. Temperature of alteration is on average 275ºC. This type of alteration is interpreted as a transitional alteration style due to a temperature increase and a change of fluid chemistry to a more Fe and Mg and K poor composition.

Group 5: Strongly enriched in Fe and Mg and strongly depleted K, Ca and Na. Chlorite is abundant while minor white mica, which is relatively low Al-rich is present in about 30% of the samples. Temperature of alteration is high (about 325ºC). The type of alteration that has affected the rocks in this group is interpreted as high intensity alteration due to high temperature and Fe and Mg rich fluids and high water/rock ratios. High temperature and high Mg and Fe activities favour the formation of chlorite over white micas.

Group 6: Strongly enriched in Fe and Mg and strongly depleted in K, Ca and Na. The style of alteration is similar to group 5. However minor white mica is present and temperature of alteration is slightly lower (275ºC). The samples of this group are derived from felsic volcanic rocks. This type of alteration is interpreted as high intensity alteration due to high temperature and Fe and Mg rich fluids and high water/rock ratios.

The distribution of alteration groups, their relationship to Kangaroo Caves deposits suggest that the alteration zones result from seawater-rock interaction, at increasing temperatures toward the subvolcanic intrusion, whereas transgressive alteration (group 5 and 6) zones mark the part of evolved seawater as it is returned to the seafloor, they are discharge zones (K depletion). Transgressive alteration zone in the Kangaroo Caves is completely feldspar destructive. Discharge zone is considered to be the center a hydrothermal connection cell, named hydrothermal vent. Discharge zone is surrounded by recharged zone (groups 1, 2 and 3), which is interpreted by white mica distributions. Group 4 represents transitional alteration. The coeval relationship of the hydrothermal vent and recharge zones indicate the Kangaroo Caves hydrothermal alteration system (Figure 2.7) [5].

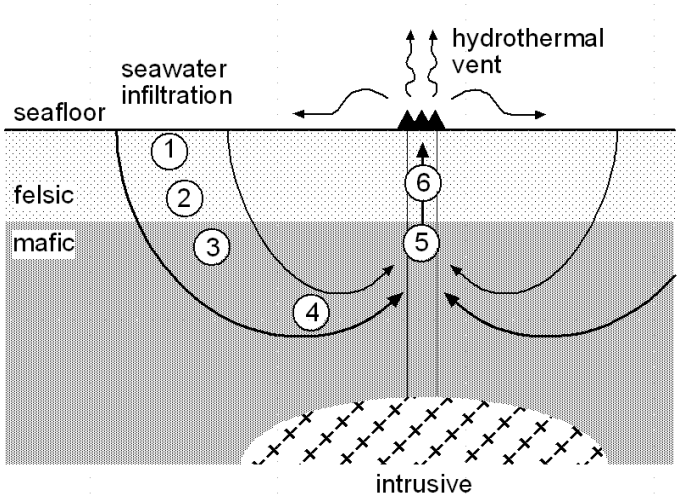

Figure 2.7: Simplified Model of Kangaroo Caves hydrothermal alteration system (Source [5]).

Another cross section (Figure 2.8) through an entire alteration system in Kangaroo Caves by Brauhart illustrates the development of VhMS mineralisation at the top of the volcanic pile and shows the broad corridor of feldspar-destructive alteration below volcanogenic massive sulfide mineralisation [3].

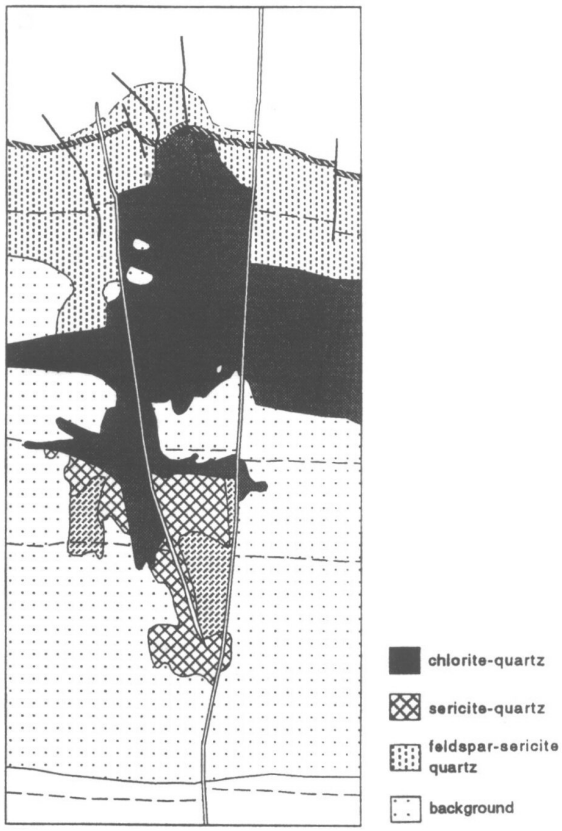

Figure 2.8: Schematic alteration sections through the Kangaroo Caves [3]

2.3. Mineralisation in the EPGGT

Mineralisation events in the North Pilbara terrain of Western Australia occurred between 3490 and 2700 Ma and include the oldest examples in the world of many ore deposit types [10].

Most of the mineralisation in the EPGGT lies predominantly within the greenstone belts that that surround the large ovoid granitoid complexes. Most occurrences are Archaean, epigenetic vein and hydrothermal gold, but they also include syngenetic, felsic volcanic-related base metal mineralisation [9]. In the EPGGT, deposits of VhMS are hosted by proximal felsic volcanic and volcanoclastic rocks, while exhalative base metal deposits are hosted by more distal volcanoclastic sedimentary rocks (Figure2.9) [9].

Base metal (VhMS) – Copper, Lead, Zinc (silver, gold)

In the Panorama area a group of related Cu-Zn deposits and prospects lies within the predominantly felsic volcanic and volcanoclastic Kangaroo Caves Formation of the Sulphur Springs Group, within the Panorama greenstone belt [9].

The two main deposits, Sulphur Springs Zn-Cu and Kangaroo Caves Zn-Cu and three prospects Breakers, Anomaly 45 and Roadmaster lie near the top of the Sulphur Springs Group and are evenly distributed at about 6 km intervals around the Strelley Granite.

At Sulphur Springs and Kangaroo Caves the sulphide assemblage is made up of pyrite, low-Fe sphalerite, chalcopyrite, and galena, with minor tennantite and arsenopyrite in some intersections.

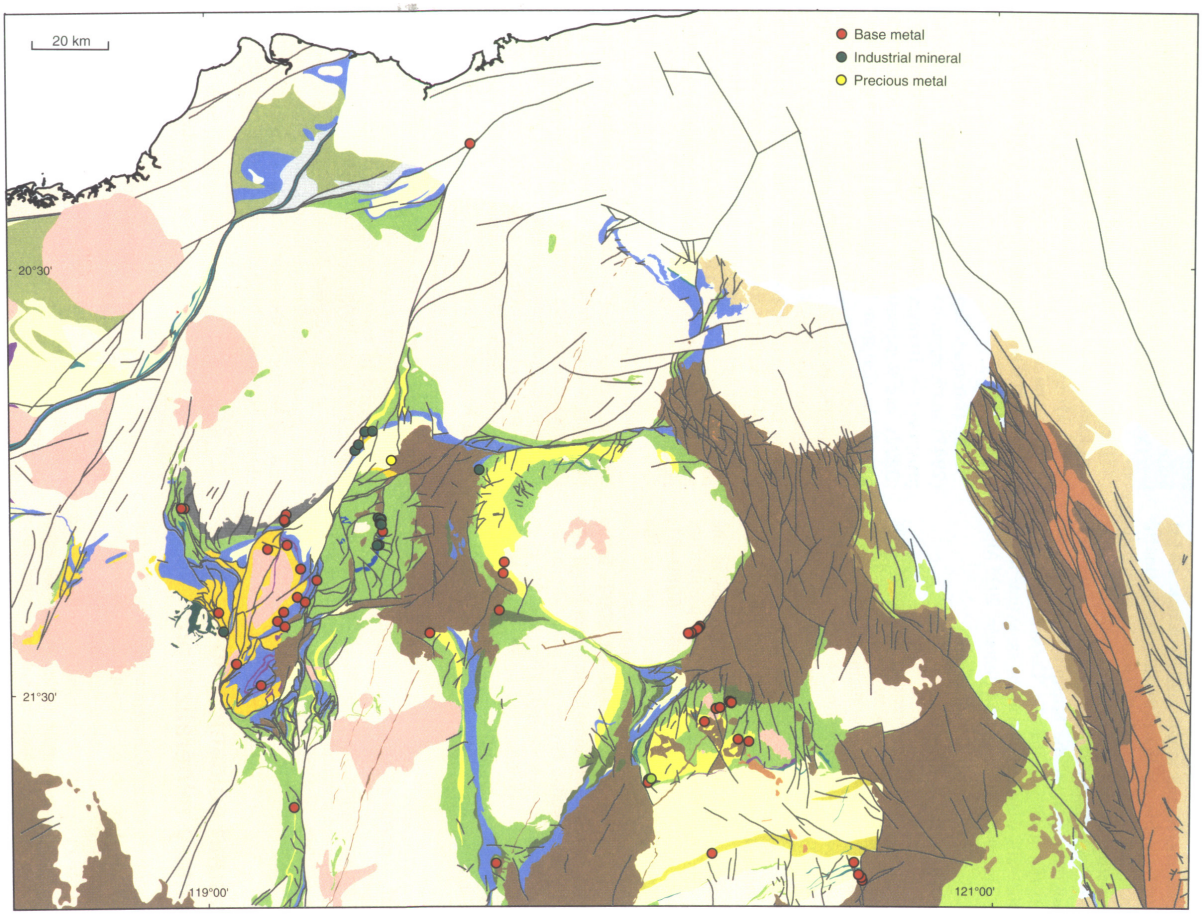

Figure 2.9: Distribution of stratabound volcanic and sedimentary mineral occurrences in the EPGGT [9]

CHAPTER 3: Datasets and Methodology

3.1. Introduction

The aim of this chapter is to give an overview of available data sets and methodology of this research.

3.2. Datasets

The spatial datasets used in this research are:

- Landsat TM imagery
- K channel of airborne gamma-ray spectrometry
- Various geological maps
- Mineral occurrence maps

3.2.1. Landsat TM imagery

The Landsat TM imagery used in this research was resampled to UTM projection and by 25 meters pixel size. This data potentially provides information on the presence of white mica and other phyllosilicates, which is one of the indicators for the presence of hydrothermal alteration systems.

The Thematic Mapper (TM) sensor is able to acquire seven bands of imagery, ranging from the visible part of the spectrum to the mid-infrared part of the spectrum. One thermal band is also included. The wavelengths of the spectrum captured by the TM sensor range from 0.45 to 12.5µm. Radiometrically, the TM sensor has a quantization range of 256 digital numbers (8 bits), which permits observation of small changes in radiometric magnitudes in a given band, and sensitivity to changes in relationships between bands [11].

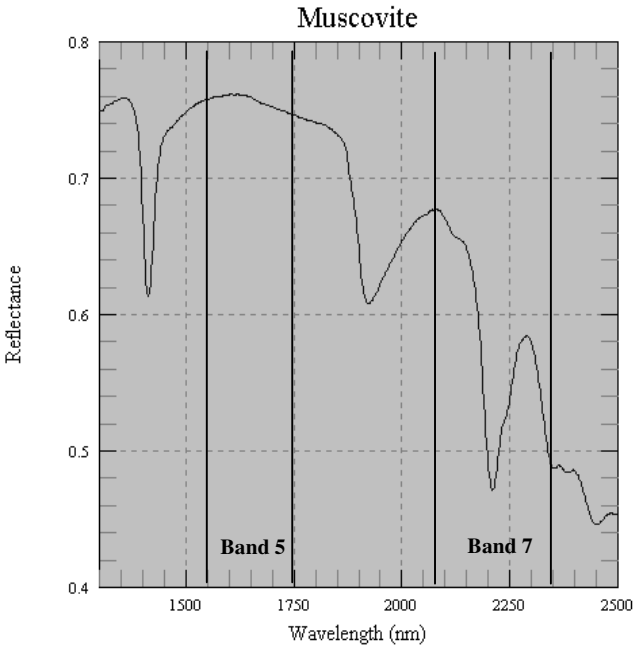

Figure 3.1: Reflectance spectra of white mica

The band 5 and 7 from Landsat TM imagery were selected for detecting white mica abundance in this study based on the reflectance spectra of white mica (Figure 3.1) in these bands.

3.2.2. Airborne gamma-ray spectrometry

The gamma-ray spectrometry data were obtained from GSWA [12] and collected under the project number 649 in 1996. The survey name was Marble Bar and flight line space was 400 m.

Data representing the K channel of airborne gamma ray spectrometry image were used by this research to map zone of K depletion, which can indicate presence of discharge zones that are related to hydrothermal systems. The data was also resampled to UTM projection and by 25 meters pixel size.

3.2.3. Geological map data

Two geological vector data sets were used in this study:

1. A published digital geological map of North Shaw [13] at 1:100 000 scale, was used to analyse the hydrothermal alteration system of Kangaroo Caves.
2. A regional geological digital data, which was produced by the North Pilbara Synthesis GIS (1997-2000) Project [2] was used during the detection of hydrothermal alteration system in the EPGGT. This geological map (granite/greenstone) was derived from interpretation of 1:100000 scale aeromagnetic and gravity data by P. Wellman and R.S. Blewett. Up to four presentation of each 1:100000 sheet area of the 400 m flight line-spacing data supplemented regional gravity images were used for interpretation. The 1500 m flight line-spacing data were used in the south, southwest east. The map is an attempt to consistently describe the granitoids in terms of their magnetic character (high, medium, low, flat) and greenstones into their basic rock type (lithology) [2].

3.2.4. Mineral occurrences data

Published regional mineral occurrences data [9] were used to validate results of regional predictive modelling carried out in this study. Information on mineral occurrences such as deposit name, status of deposit and locations are given in related tables.

3.2.5. Dataset coordinate systems and map projections

A common coordinate system for all raster data layers is important for integrated data analysis. In this research, the raster data sets were resampled to a common map projection. The coordinate system, map projections, ellipsoids, datum and pixel sizes of the various datasets used in this study are given in below:

Table 3.1: Coordinate system, map projection and pixel size of the datasets.

Datasets	Type of data	Coordinate system	Projection	Ellipsoid	Datum	Pixel size (m)
Landsat TM images	*Raster*	*AMG 66*	*UTM*	*Australian National / South zone 50*	*Australian Geodetic 1966*	*25 x 25*
Airborne Gamma ray Spectrometry image	*Raster*	*AMG 66*	*UTM*	*Australian National / South zone 50*	*Australian Geodetic 1966*	*25 x 25*
Geology (detailed and regional)	*Vector*	*Geographic (LatLong)*	-	*WGS 84*	*WGS 1984*	-
Mineral occurrences	*Vector*	*Geographic (LatLong)*	-	*WGS 84*	*WGS 1984*	-

3.3. Methodology

3.3.1. Research scheme

The main research scheme of the thesis is given in Figure 3-2, which is explained as follows.

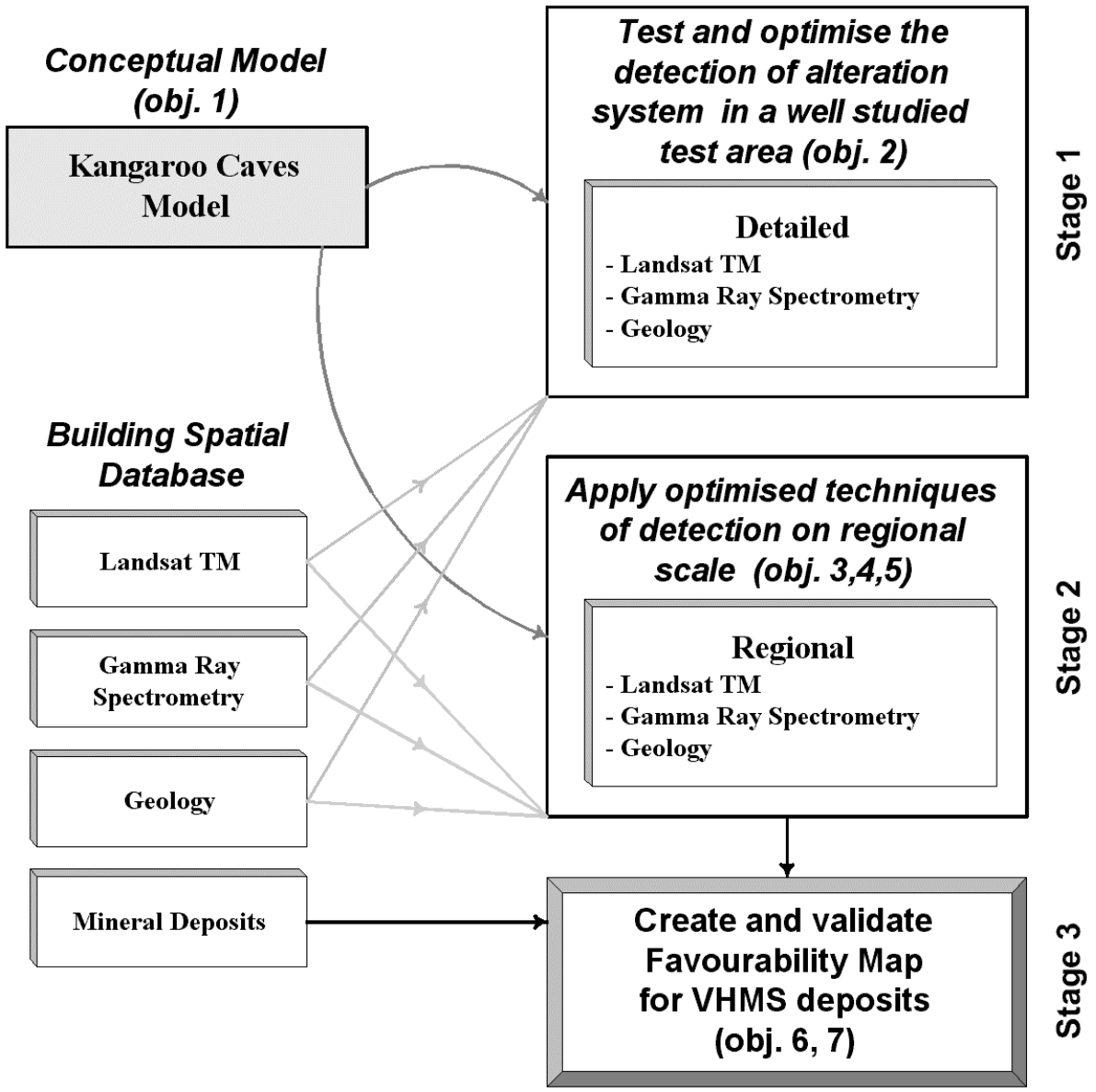

Figure 3.2: The research methodology flowchart of the thesis.

First stage

The first stage that relates with second sub-objective is to test and optimise the detection of alteration system in a well-studied test area (Kangaroo Caves). The steps of data processing applied for each data set are summarised below.

- To process and enhance Landsat TM imagery for mapping white mica distribution.
- To process and enhance gamma-ray spectrometry imagery for mapping enrichment and depletion of potassium.
- To test and optimise detection of the various hydrothermal alteration facies using the enhanced images.

Second stage

The second stage relates with third, fourth and fifth sub-objectives. The optimised methods of for detection of the alteration system Kangaroo Caves are applied to the rest of study area. The steps of these stages are:

- To process and enhance Landsat TM imagery for mapping white micas and other phyllosilicates.
- To process and enhance gamma-ray spectrometry imagery for mapping enrichment and depletion of potassium.
- To look for areas with similar spatial distribution of white micas and potassium as the Kangaroo Caves system.
- To identify possible hydrothermal alteration systems similar to that Kangaroo Caves system.
- To identify possible discharge zones and VhMS deposits.

Third stage

In this stage the map of potential VhMS deposit locations are validated using known mineral deposit data.

3.3.2. Image processing and enhancement

The following of image processing and enhancement are used:

Spectral Band Ratio

Digital data have an advantage over analogue photographic information in that particular spectral attributes of interest can be enhanced.

Dividing brightness values, pixel by pixel, of one band by another, creates a ratio.

Ratio images are usually derived from the absorption/reflection spectra and thus often provide information on the mineralogical composition of the target. They enlarge small differences between various rock types, which could not be identified at original color composites. They are therefore applied in mineral exploration. Combination of Landsat TM ratios are used for mineral type detection like for example Red 5/7, Green 5/4 and Blue 3/1, integrating the ratios for iron oxide (3/1), for clay minerals (5/7) and ferrous minerals (5/4). Ratios are also used to reduce relief induced illumination effects [14].

Ratios are used to create output images by mathematically combining the DN values of different bands. They could be generated through arithmetic operations like:

$$(\text{Band X} - \text{Band Y})$$

or as ratios of band DN values:

$$\text{Band X} / \text{Band Y}$$

or more complex:

$$(\text{Band X} - \text{Band Y}) / (\text{Band X} + \text{Band Y})$$

The output images resulting from ratio operations should generally be created in floating point format to preserve all numerical precision, since usually A is not much greater than B and the data range might only go from 1 to 2 or 1 to 3. For cases in which A<B integer scaling would always result in 0 and all fractional data would be lost. Faust (1989) provide an approach to handle the entire ratio range by:

$$\text{Ratio} = \text{ATAN}(A/B)$$

representing the range smaller and larger than 1 pretty well [14].

The inverse tangent of the ratio of band 5 over 7 (ATAN (band5/band7)) was calculated to enhance the presence of white micas.

Normalisation

In order to compensate for the differences in K and white micas between various lithological units in the study area the ratio images and K images were normalised by lithology. Using this method the variation within lithological units is enhanced which enables detection of patterns related to hydrothermal alteration.

An ILWIS (Appendix A) script was used to normalise images in this study. An image will be normalised using another classified map containing geological units. Normalisation here is based on the division of digital number of the enhanced image minus the average value (Avg) in a certain geological unit divided by the standard deviation:

$$\text{Normalised Map} = (DN - Avg) / Stdev$$

CHAPTER 4: Remote Detection of Kangaroo Caves Alteration System

4.1. Introduction

In this chapter, the remote detection of the Kangaroo Caves alteration system using Landsat TM imagery and the K channel of gamma-ray spectrometry was optimised. The location of the test area is shown on the Figure 4.1.

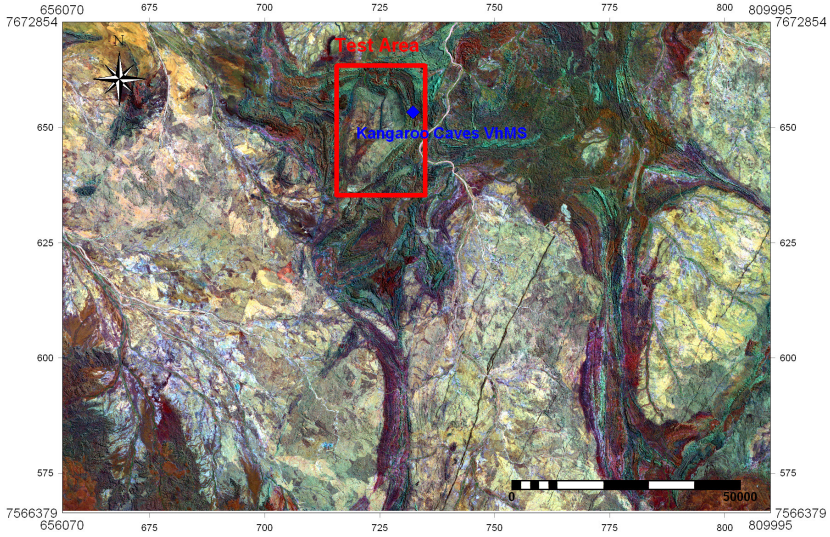

Figure 4.1: Test Area location map (Landsat TM imagery, band combination 7,4,2 as RGB).

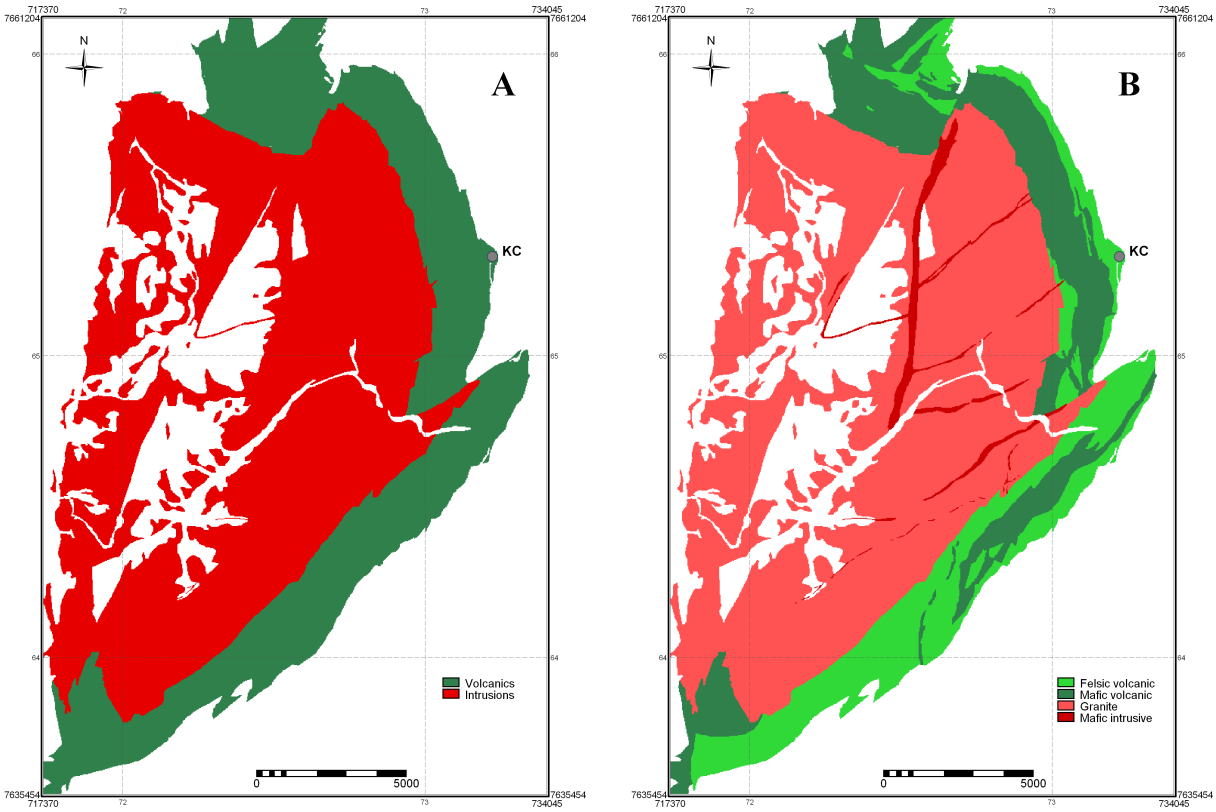

Figure 4.2: Test area: (**A**) unified geological map; (**B**) classified geological map.

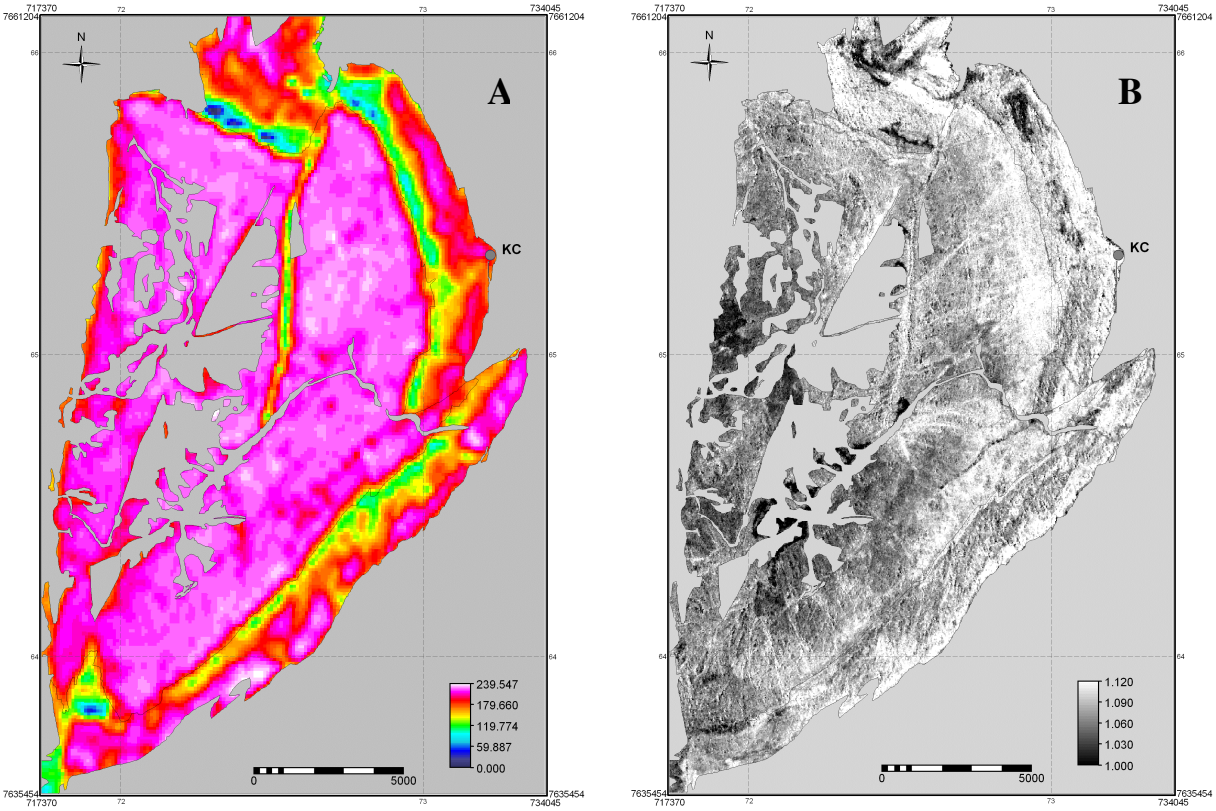

Figure 4.3: Test area: (**A**) potassium image; (**B**) ratio image.

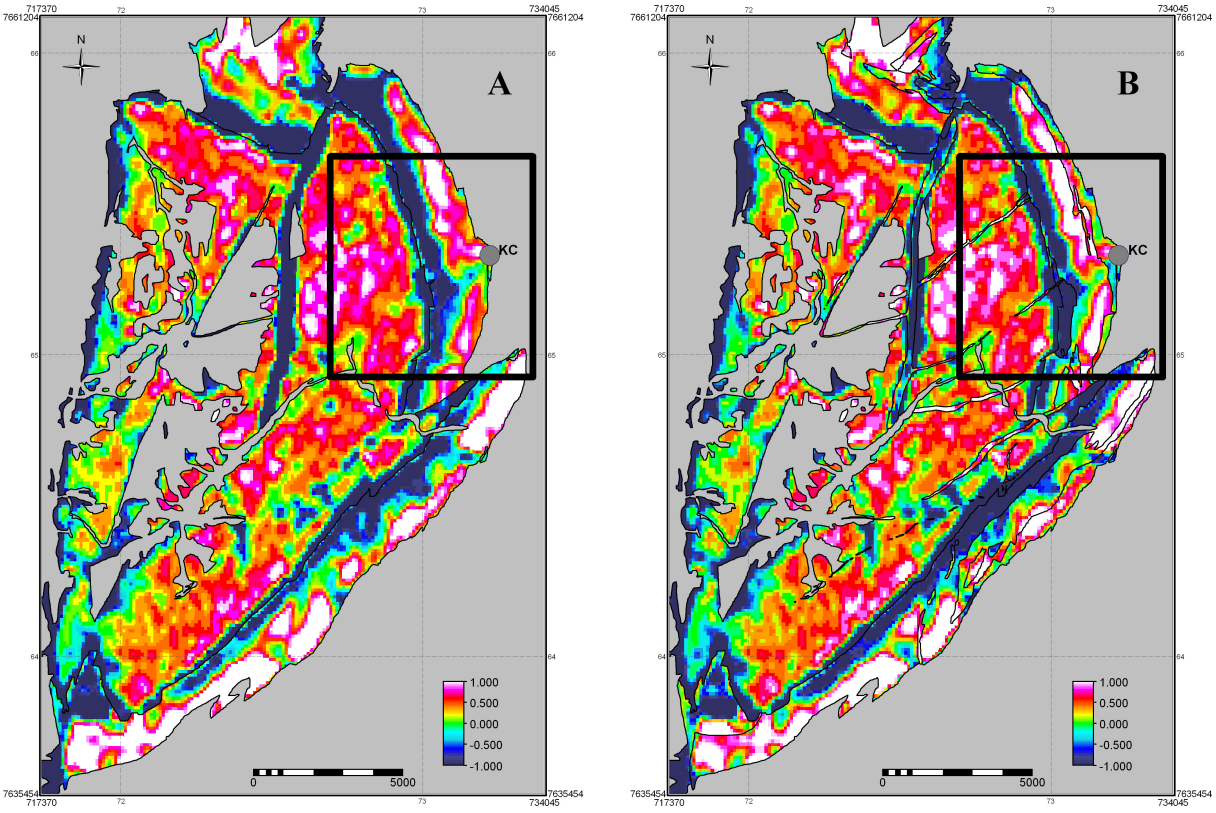

Figure 4.4: Test area: (**A**) normalised potassium image, based on unified geologic map in Figure 4.4A; (**B**) normalised potassium image, based on classified geologic map in Figure 4.4B. Thin black lines are the lithological boundaries and area in thick black line is study area.

The K channel image and the ratio image (ATAN(5/7)) of Landsat TM were normalised to lithology. Normalisation was done using two levels of differentiation of rock units (Figures 4.2A and 4.2B). The sequence of the volcanic rocks and intrusions is the major key used to detecting hydrothermal alteration in this research such that sedimentary and other type of rocks were excluded for the normalisation, which are considered geologically unfavourable to host VhMS deposits.

In the first lithological map only volcanics and intrusions were differentiated (Figure 4.2A). The second map was classified as the felsic and mafic rocks between those units (Figure 4.2B). Other geological units such as sediments and unclassified units that are the greenstone and rock were removed for those maps.

Figure 4.3A shows the unenhanced potassium image of the test area, which indicates that potassium concentration is highest towards top of the volcanic sequence and in the granitic intrusion. Potassium depletion is not clearly seen in the Kangaroo Caves deposit site. The image gives the trend of potassium distribution in the area but does not indicate depletion and enrichment of potassium.

In the ratio image (ATAN (band5/band7)) shown in Figure 4.3B, bright pixels indicate white mica abundance but only gives general information. In the felsic volcanic rock, white mica can be seen more distributed than other geological units. But it is difficult to extract hydrothermal alteration from this ratio image.

4.2. Airborne gamma-ray spectrometry image

The unenhanced potassium image shown in Figure 4.3A was normalised based on each geological map shown in Figure 4.2A and 4.2B and the results are shown respectively in Figures 4.4A and 4.4B. These normalised maps were stretched to the range –1 to 1 to enhance the contrast of the maps.

Generally, high potassium concentrations occur in felsic intrusions. In volcanic rocks, there is a general trend for increasing potassium content from mafic to felsic volcanic rocks. That means felsic volcanics are potassium rich while mafic volcanics are potassium poor (Figure 4.4).

Strong potassium depletion occurs at the bottom of the volcanic sequence near the contact with the intrusion. Along the top of the volcanic sequence, where felsic volcanics occur, there is almost continuous potassium enrichment, which is crosscut by a zone of potassium depletion, underlying the Kangaroo Caves deposit (Figure 4.4A). The zone of potassium depletion continues down into the intrusions.

The main technique of the normalisation was to calculate average concentration of the potassium in each of the lithological units, which were used during normalisation. Figure 4.5 shows those average values for each map from normalisation.

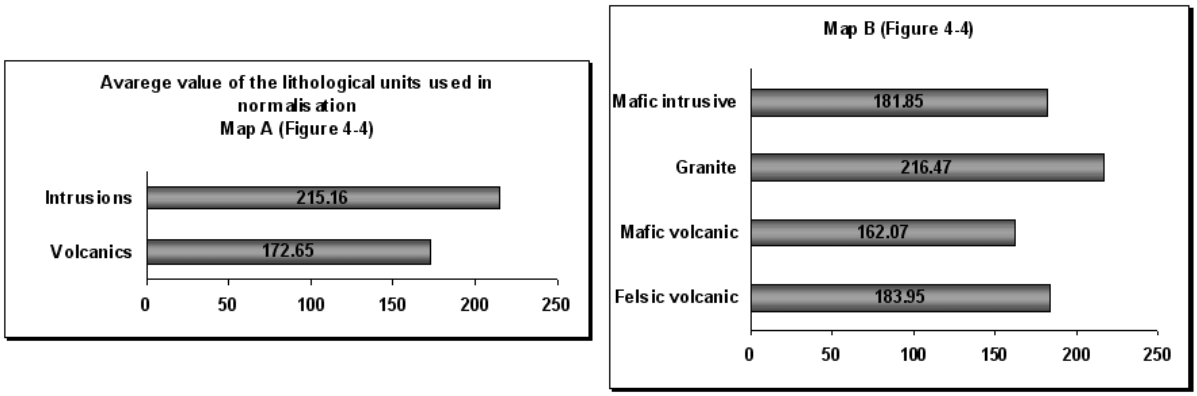

Figure 4.5: Average values of potassium in lithological units used in normalisation.

The average potassium value is higher in the intrusions than in the volcanics, which depends on the mineralogical compositions of the rock types.

Therefore, for the normalisation of potassium gamma-ray image, the unified geology map was suitable to interpret potassium concentration. The distribution of potassium depletion and enrichment is clearer and continuously appear in the normalised image by unified geology than in the normalised image by classified map.

4.3. Landsat TM imagery

The normalisation method was applied to the ratio image (Figure 4.3B) using the unified lithologic map (Figure 4.2A) and the classified lithologic map (Figure 4.2B) and the results are shown in Figure 4.6. The normalised ratio images (Figure 4.6) represent potential abundance of white mica in each geological unit based on average white mica distribution in the differentiated lithology of the test area.

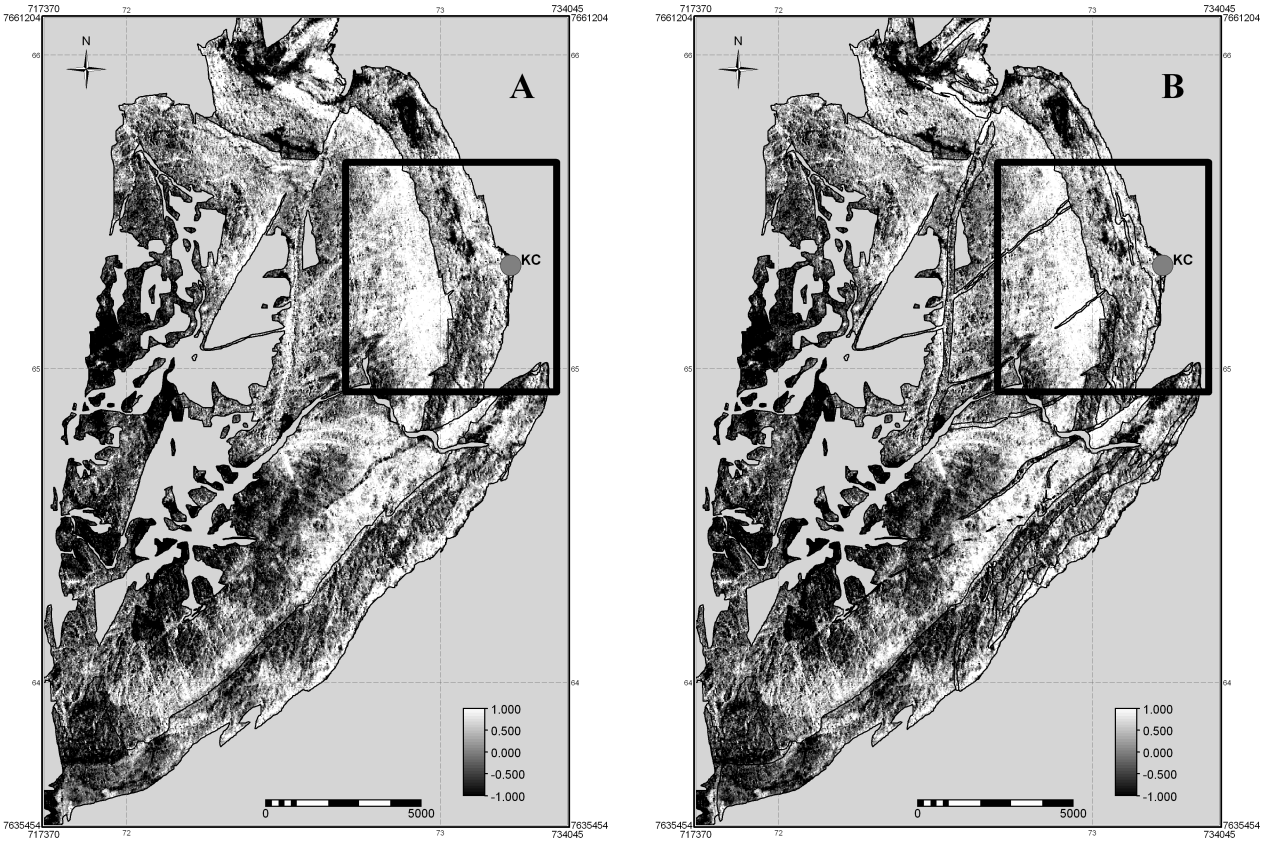

Figure 4.6: Test area: (**A**) normalised ratio image, based on unified geologic map in Figure 4.4A; (**B**) normalised ratio image, based on classified geologic map in Figure 4.4B. Thin black lines are the lithological boundaries.

Generally, white mica is enriched in the top of the volcanic sequence, which means felsic volcanic unit contains more white mica than mafic volcanic unit. Also, near top of the intrusion that contact with bottom of the volcanic sequence, there is strong enrichment in white mica (Figure 4.6). This enrichment is strongest in the area underlying the Kangaroo Caves deposit. But in the some part of mafic volcanics, there are white mica enrichments probably due to influence of hydrothermal alteration.

Figure 4.7 shows average ratios in each lithological unit used in the normalisation. In felsic volcanic rocks, the average ratio is higher than in other rocks, which conforms to term of mineral

consists of felsic rock (map B). The volcanic unit, which was normalised with unified lithology map (map A), has high average ratios.

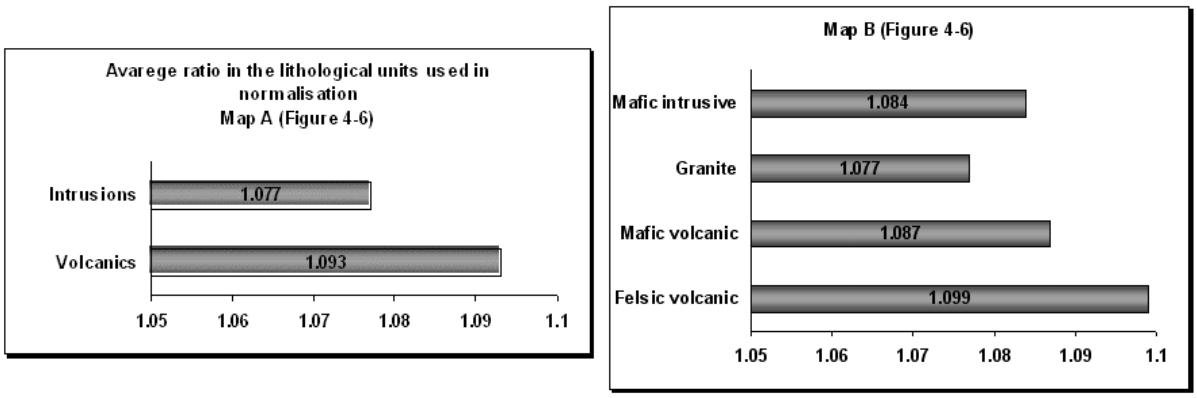

Figure 4.7: Average ratios in lithological units used in normalisation.

4.4. Discussion

The following parts of the hydrothermal alteration system of Kangaroo Caves were detected:

1. Conformable alteration related to see water infiltration

The grey line in Figure 4.8 indicates the direction of infiltrating seawater. The volcanic rocks along this line are hydrothermally altered and white mica is the dominant alteration mineral. The altered rocks are rich in potassium (Figure 4.9A). The potassium concentration in the felsic rocks has not significantly changed due to the hydrothermal alteration. The potassium concentration of the white mica altered mafic volcanics has increased due to the hydrothermal alteration event compared to unaltered mafic rocks. About 200-400 meters below the paleo-seafloor, both potassium and white concentration decrease. The zone of high potassium and white mica content is similar to the conformable or recharge related alteration facies described by Van Ruitenbeek [5] and the feldspar-sericite-quartz alteration by Brauhart alteration classes [3].

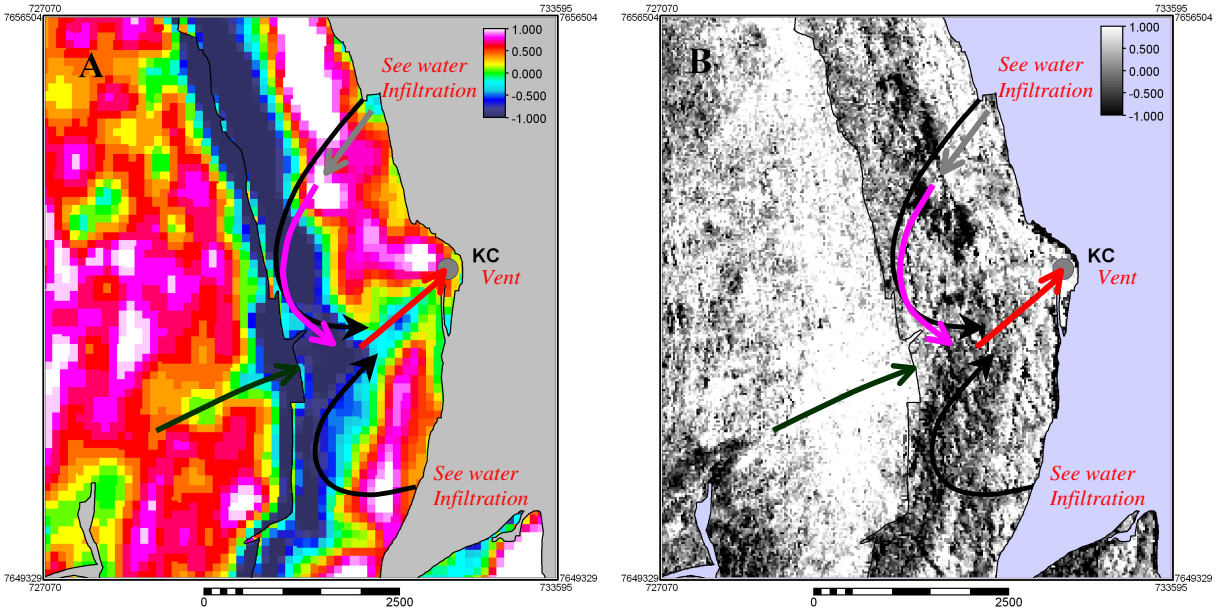

Figure 4.8: Kangaroo Caves area: (**A**) normalised potassium image; (**B**) normalised ratio image.

2. Transitional alteration

The magenta line in Figure 4.8 indicates fluid flow deeper in the volcanic sequence where temperatures are higher K concentration and white mica concentration is lower than in the recharge related facies. This alteration facies is similar to the transitional alteration from feldspar-sericite-quartz alteration to chlorite-quartz alteration by Brauhart [3] (Figure 2.8) and group 4 in Figure 2.7.

3. Transgressive alteration related to fluid discharge

The red arrow in Figure 4.8 indicates where high temperature fluids rise and are discharge at the paleo-seafloor. This zone is characterized by a strong potassium depletion that crosscuts the stratigraphy and the potassium enrichment in the top of the volcanic sequence. Depletion in white mica is not very prominent in the normalised ratio image. The potassium depletion zone is similar to alteration facies 5 and 6 in Figure 2.7 and is similar to the transgressive chlorite-quartz alteration described by Brauhart (Figure 2.8). Potential VhMS deposits are expected where this zone intersects the paleo-seafloor.

4. Transgressive alteration in the underlying felsic intrusion

The green arrow indicates hydrothermal fluid flow in the top of the felsic intrusion (the Strelley Granite). The granite is hydrothermally altered and enriched in white mica and depleted in potassium directly below the Kangaroo Caves deposit. This zone coincides with the sericite and chlorite-quartz alteration facies described by Brauhart [3] (Figure 2.8).

4.5. A Model to Detect Hydrothermal Alteration Systems

This section presents models of potassium and white mica distributions in a geological setting similar to that of Kangaroo Caves, which is a bi-modal volcanic greenstone belt underlain by a felsic granitic intrusion. The first model represents potassium and white mica variation in a geological background setting without hydrothermal alteration. The second shows modification of the potassium and white mica distribution due to hydrothermal alteration. These models will be used in chapter 5 to detect other hydrothermal systems in the EPGGT.

Without hydrothermal activity

Figure 4.9 shows simplified models of (A) the variation in potassium and (B) white micas in a geologic background setting without effect of hydrothermal alteration.

The volcanic, pile consisting of mafic volcanics (e.g., basalt) at lower portions and of felsic volcanics (e.g., rhyolite) at upper portions, is underlain by felsic intrusive rocks (Figure 4.9). Since felsic volcanics, commonly form toward the end of a volcanic cycle, they have very high silica content and are rich in potassium. Felsic intrusives (e.g., granite) have more or less the same potassium (and silica) content as their volcanic equivalent (Figure 4.9A).

Volcanic rocks in the study area are low-grade metamorphosed. Felsic volcanic rock may contain white mica, which was derived from feldspar. White mica may also occur along the contact between granite and mafic volcanics, as a result of contact metamorphism (Figure 4.9B).

With hydrothermal activity and hydrothermal alteration systems

Figure 4.10 shows models of modifications of the distribution of (A) potassium and (B) white mica as a result of hydrothermal activity in the volcanic pile and underlying felsic intrusion.

The architecture of the hydrothermal system of Kangaroo has been described in previous section. It is composed of 3 alteration zones in the volcanic sequence: (1) the recharge zone, (2) transitional zone and (3) discharge zone in the study area. Another alteration zone is present in the underlying felsic intrusion.

1. In the recharge related alteration facies the potassium concentration and the white mica is relatively high. This type of hydrothermal alteration results in an increase of potassium in mafic volcanic rock and an increase in white micas in both mafic and felsic volcanic rock.
2. In the transitional alteration facies both potassium concentration and white micas content is low. There are no significant changes in both variables due to hydrothermal alteration.
3. In the discharge related alteration facies potassium concentration is very low which results in a strong depletion that cross cuts the conformable zone of potassium enrichment in the upper part of the volcanic sequence. Also white mica content is relatively low but this is not as clear as the potassium depletion. The discharge zone ends where it intersects the paleo-seafloor at the top of the volcanic sequence where the hydrothermal fluids discharge at hydrothermal vents and VhMS deposit are likely to be deposited.
4. The hydrothermal alteration in the underlying felsic (granitic) intrusion is indicated by a zone of potassium depletion directly beneath the discharge zones and a broader zone of white mica alteration.

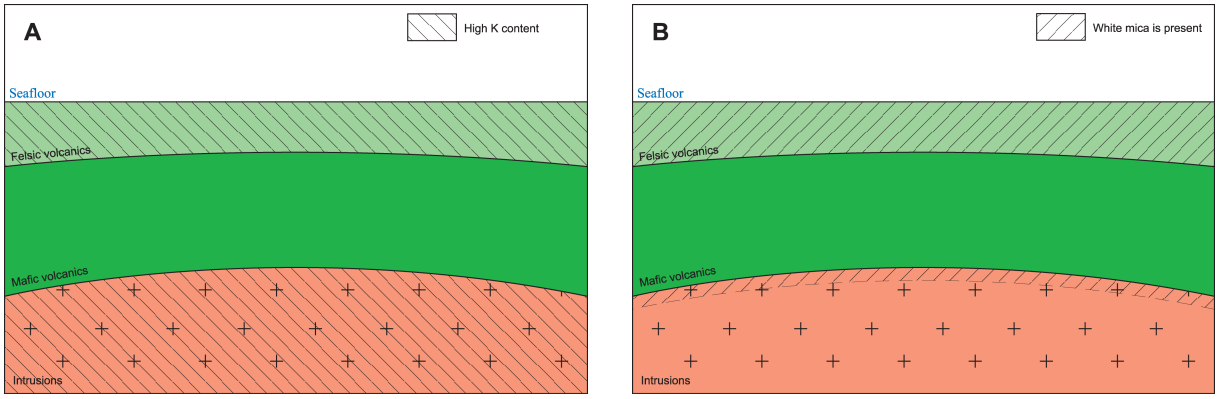

Figure 4.9: Without hydrothermal activity: (**A**) potassium distribution; (**B**) white mica distribution.

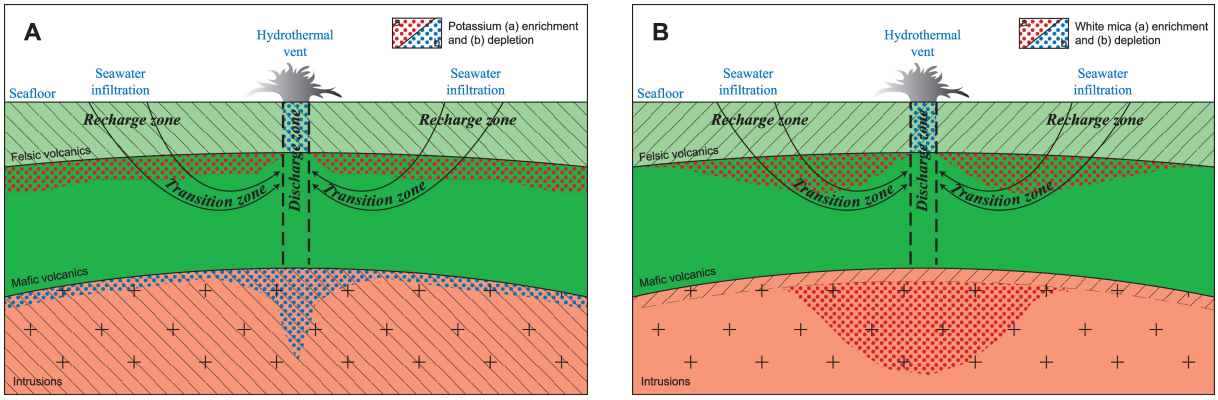

Figure 4.10: With hydrothermal activity: (**A**) potassium distribution; (**B**) white mica distribution.

CHAPTER 5: Remote Detection of Hydrothermal Alteration Systems in the East Pilbara

5.1. Introduction

Based on the results of chapter 4, the aim of this chapter is to detect similar hydrothermal alteration systems in other parts of the East Pilbara granite greenstone terrain. In general, areas with a similar geological setting as the Kangaroo Caves area normalised potassium and Landsat ratio images were produced. Each of the areas consists of a volcano-sedimentary sequence and is underlain stratigraphically by a felsic intrusion.

5.2. The East Pilbara Granite Greenstone Terrain

Figure 5.1 shows a simplified geological map of the EPGGT. Figures 5.2 and 5.3 are, respectively, normalised K-images and ratio images based on geological units in Figure 5.1.

Several sub-areas were selected for further interpretation (Figure 5.1). They are described in the following sections. Research work is focused on four sub-areas within the study area that were possibly affected by hydrothermal activity.

Normalisation is applied to each area separately in K and ratio images. Interpretations of top of volcanic sequence and paleo seafloor level were made by comparing normalised images and false color composition image of Landsat TM imagery based on relief difference. Recharge related alteration in volcanics and alteration in intrusion of white micas are interpreted from normalised ratio images. Discharge related alteration and alteration in intrusion of K are interpreted from normalised K images. Every interpretation is done based on the model, which is discussed in section 4.5.

5.2.1. Area 1: Strelley

Normalised images of the Strelley area, including the Panorama greenstone belt, were interpreted in terms of K-enrichment and depletion (Figure 5.4A) and white mica enrichment and depletion (Figure 5.4B). 9 possible alteration systems and potential discharge zones were interpreted (Figure 5.4D and Table 5.1).

Table 5.1: Potential discharge zones in area 1 (Figure 5.4).

Potential Discharge Zones	Hydrothermal alteration				
	Volcanics			Intrusions	
	Discharge related		Recharge related	K depletion (Fig. 5.4A)	White mica alteration (Fig. 5.4B)
	K depletion (Fig. 5.4A)	White mica depletion (Fig. 5.4B)	White mica enrichment (presence) (Fig. 5.4B)		
DZ 1.1	Strong	None	Yes	Strong	Yes
DZ 1.2	Strong	Weak	Yes	Weak	Yes
DZ 1.3	Strong	Weak/none	Yes	Strong	Yes
DZ 1.4	Weak	Weak/none	Yes	Strong	Yes
DZ 1.5	Strong	Weak/none	Yes	Strong	Yes
DZ 1.6	Strong	None	Yes	Weak	Yes
DZ 1.7	Strong	Strong	Yes	Weak	Yes
DZ 1.8	Weak	Weak	Yes	Weak	Yes
DZ 1.9	Strong	None	Yes	Strong	Yes

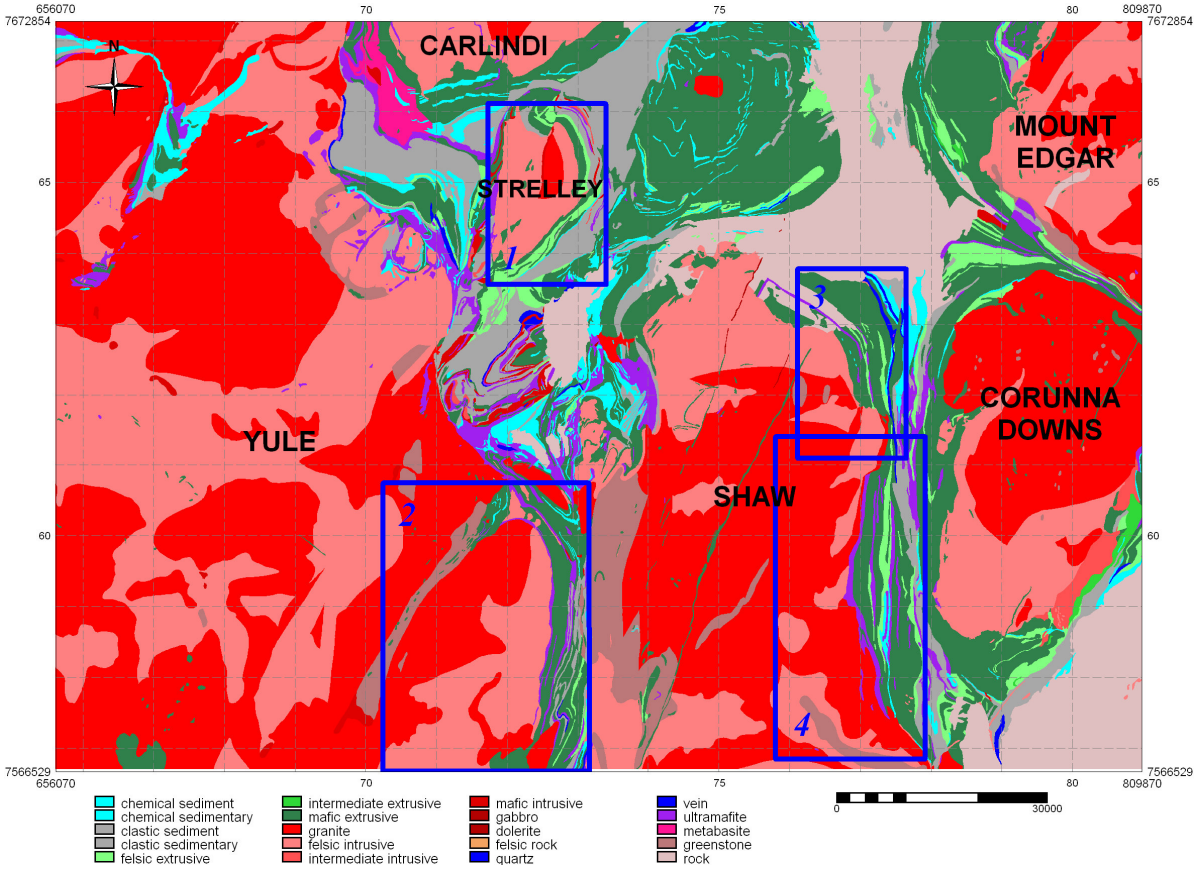

Figure 5.1: Regional geology map of EPGGT .

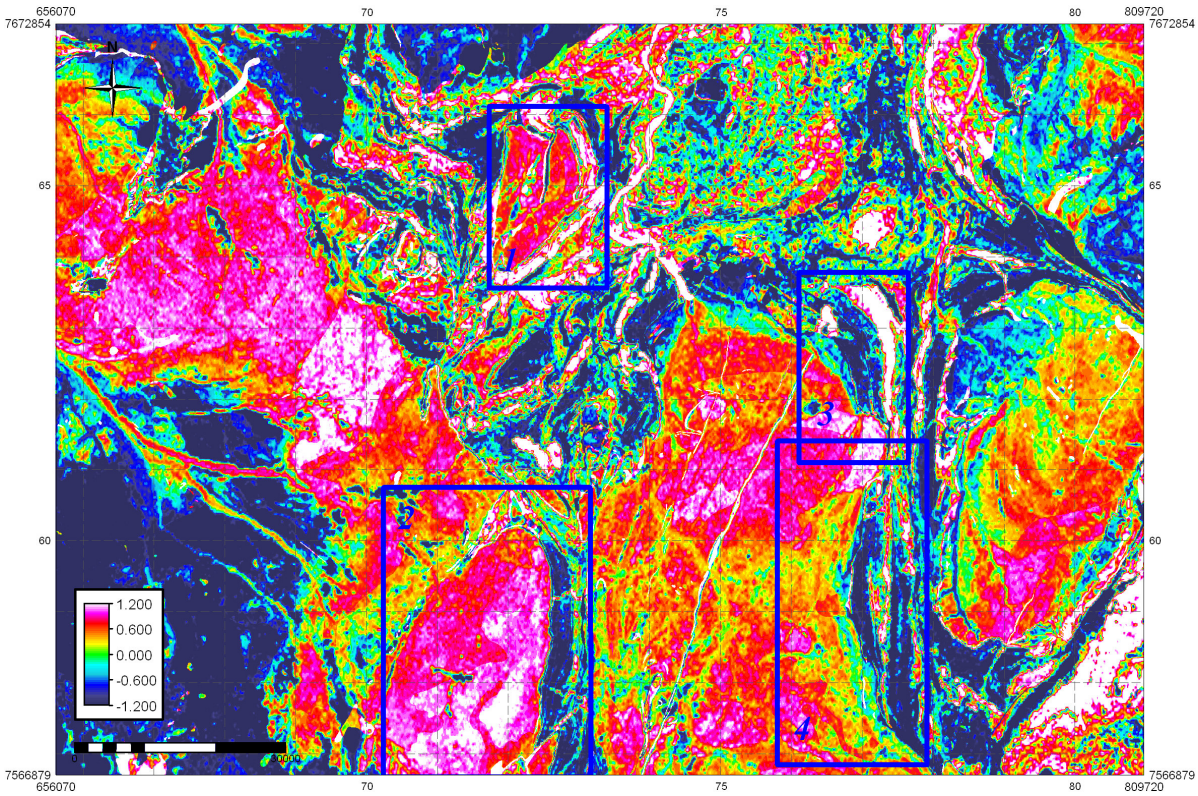

Figure 5.2: Normalised potassium image of EPGGT.

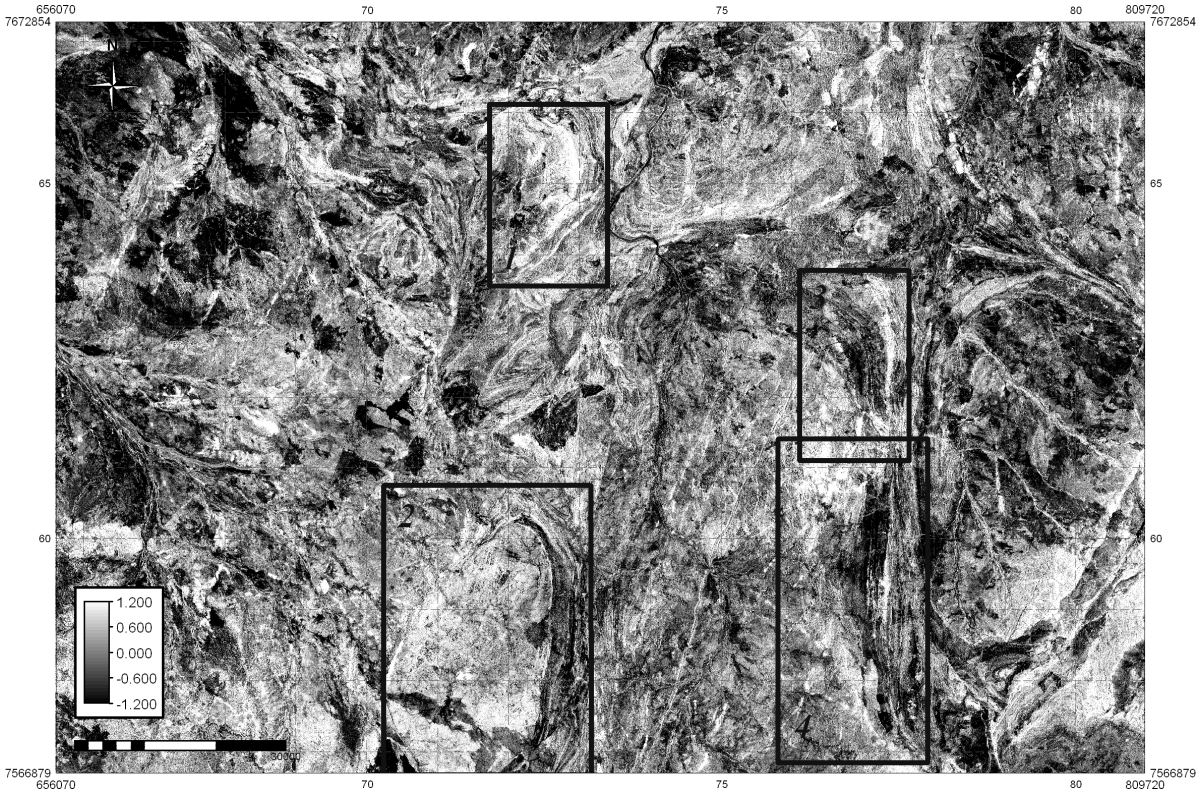

Figure 5.3: Normalised ratio image of EPGGT.

5.2.2. Area 2: Yule

Normalised images of the east-south part of the Yule granite complex and Western Shaw greenstone belt were interpreted in terms of enrichment and depletion of K (Figure 5.5A) and white mica (Figure 5.5B). The possible hydrothermal alteration systems were interpreted (Figure 5.5 D) and based on this interpretation the following 11 potential discharge zones were discovered in this area (Table 5-2).

Table 5.2: Potential discharge zones in area 2 (Figure 5.5).

Potential Discharge Zones	Hydrothermal alteration				
	Volcanics			Intrusions	
	Discharge related		Recharge related	K depletion (Fig. 5.5A)	White mica alteration (Fig. 5.5B)
	K depletion (Fig. 5.5A)	White mica depletion (Fig. 5.5B)	White mica enrichment (presence) (Fig. 5.5B)		
DZ 2.1	Weak	Strong	Yes	Strong	Yes
DZ 2.2	Strong	Weak	Yes	Strong	Yes
DZ 2.3	Strong	Strong	Yes	Strong	Yes
DZ 2.4	Weak	Strong	Yes	Strong	Yes
DZ 2.5	Weak	Weak/none	Yes	Strong	Yes
DZ 2.6	Weak	None	Yes	Strong	Yes
DZ 2.7	Strong	None	Yes	Strong	Yes
DZ 2.8	Weak	Weak	Yes	Strong	Yes
DZ 2.9	Weak	None	Yes	Strong	Yes
DZ 2.10	Weak	Strong	Yes	Strong	Yes
DZ 2.11	Weak/none	Strong	Yes	Strong	Yes

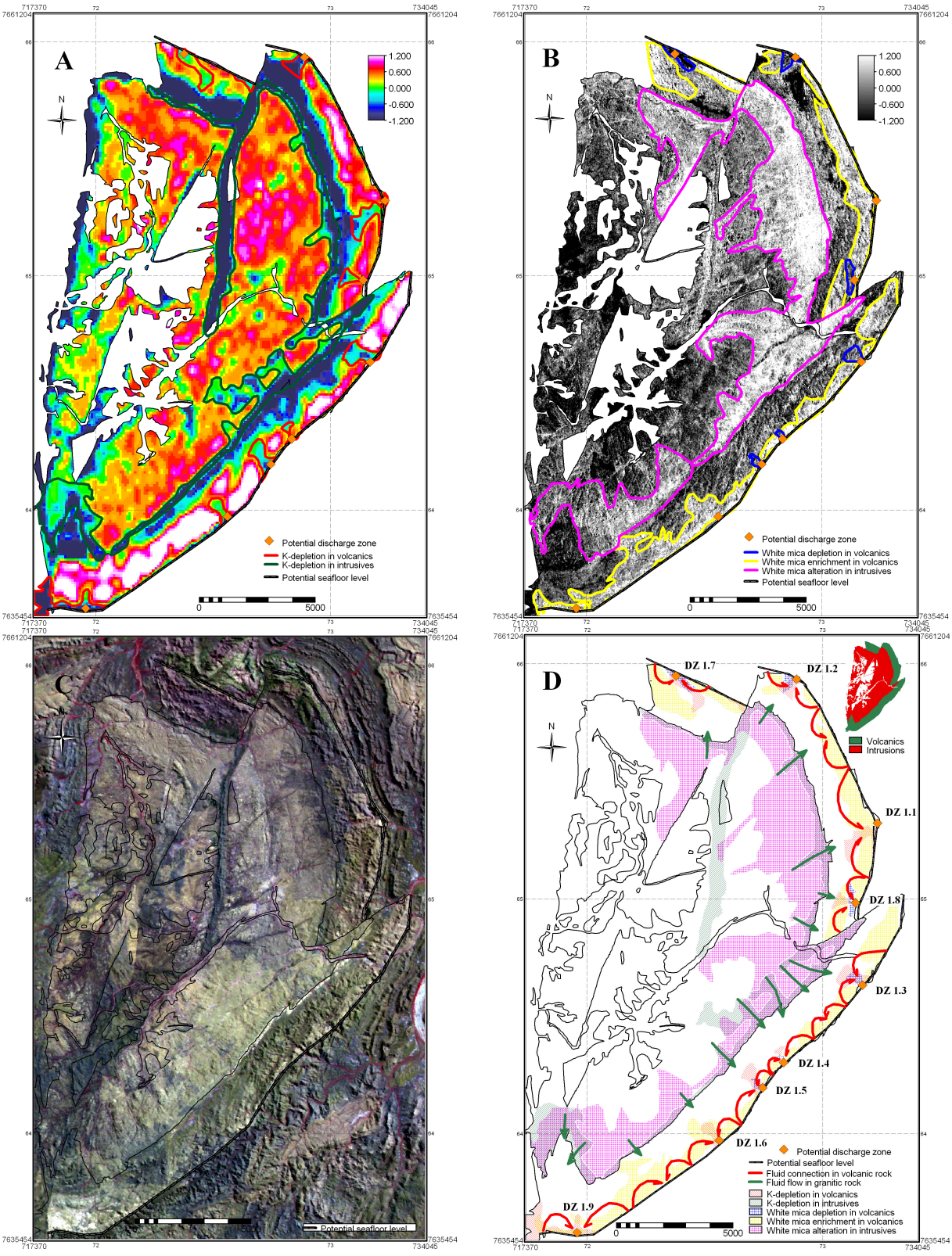

Figure 5.4: Strelley: (**A**) normalised potassium image; (**B**) normalised ratio image; (**C**) Landsat TM imagery false color composite; (**D**) hydrothermal alteration systems and lithology in inset .

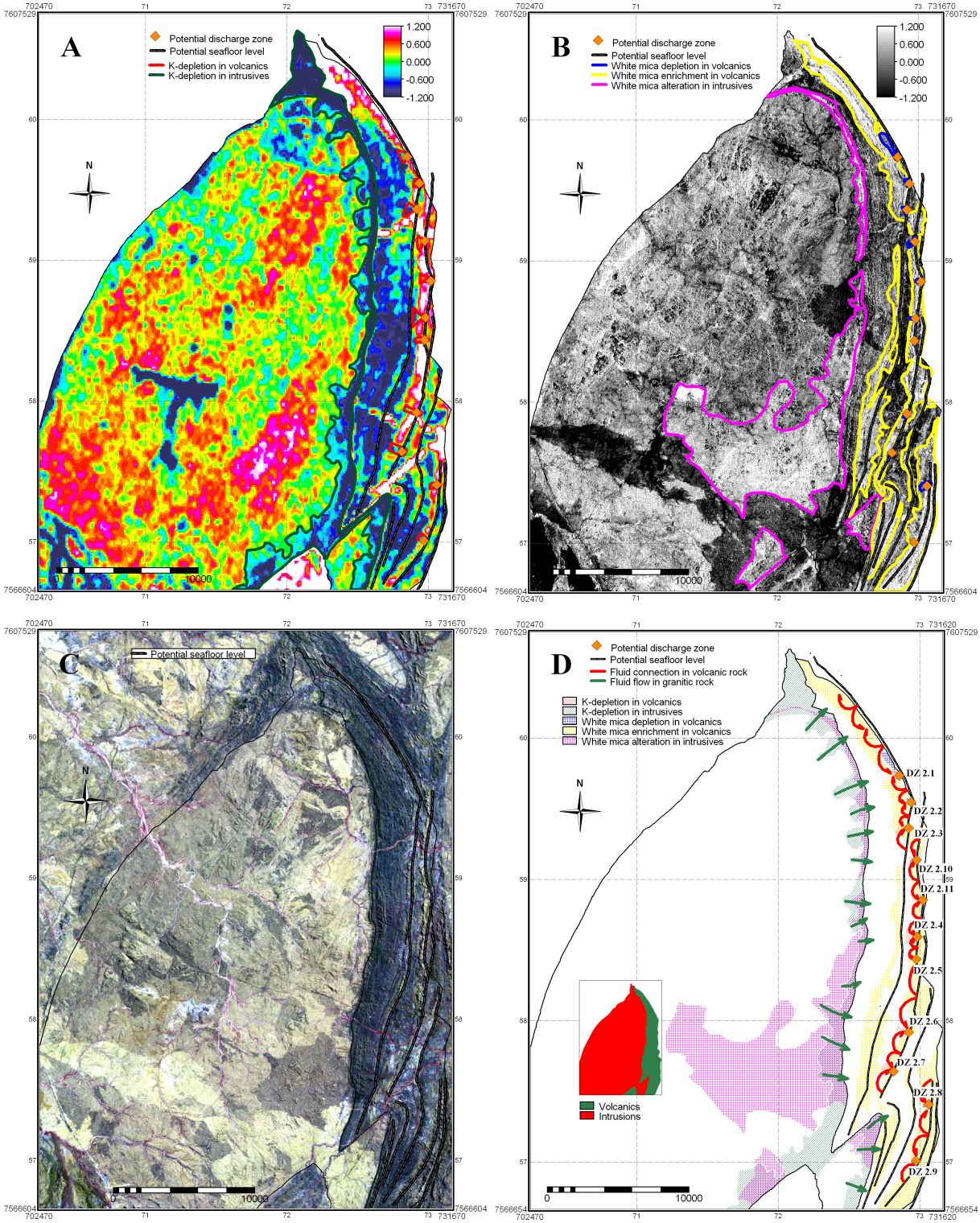

Figure 5.5: Yule: (**A**) normalised potassium image; (**B**) normalised ratio image; (**C**) Landsat TM imagery false color composite; (**D**) hydrothermal alteration systems and lithology in inset.

5.2.3. Area 3: Northern Shaw

Normalised images of the north-east part of Shaw granite complex and north part of Coongan greenstone belt were interpreted in terms of enrichment and depletion of K (Figure 5.6A) and white mica (Figure 5.6B). The following possible alteration systems were interpreted and 4 potential discharge zones were determined (Figure 5.6 D) and shown Table 5-3.

Table 5.3: Potential discharge zones in area 3 (Figure 5.6).

Potential Discharge Zones	Hydrothermal alteration				
	Volcanics			Intrusions	
	Discharge related		Recharge related	K depletion (Fig. 5.6A)	White mica alteration (Fig. 5.6B)
	K depletion (Fig. 5.6A)	White mica depletion (Fig. 5.6B)	White mica enrichment (presence) (Fig. 5.6B)		
DZ 3.1	Strong	None	Yes	Strong	Yes
DZ 3.2	Weak	Weak	Yes	Strong	Yes
DZ 3.3	Weak	None	Yes	Strong	Yes
DZ 3.4	Weak	Strong	Yes	Strong	Yes

5.2.4. Area 4: Eastern Shaw

Possible hydrothermal alteration systems (Figure 5.7D) were interpreted from normalised K image (Figure 5.7A) and ratio image (Figure 5.7B) in terms of enrichment and depletion of the K and white mica distribution in the east-south part of the Shaw granite complex and south part of Coongan greenstone belt. 14 potential discharge zones were found and described hydrothermal alteration distributions of them in Table 5.4.

Table 5.4: Potential discharge zones in area 4 (Figure 5.7).

Potential Discharge Zones	Hydrothermal alteration				
	Volcanics			Intrusions	
	Discharge related		Recharge related	K depletion (Fig. 5.7A)	White mica alteration (Fig. 5.7B)
	K depletion (Fig. 5.7A)	White mica depletion (Fig. 5.7B)	White mica enrichment (presence) (Fig. 5.7B)		
DZ 4.1	Weak	None	Yes	Strong	Yes
DZ 4.2	Weak	None	Yes	Strong	Yes
DZ 4.3	Strong	Weak	Yes	Strong	Yes
DZ 4.4	Strong	Strong	Yes	Strong	Yes
DZ 4.5	Strong	None	Yes	Strong	Yes
DZ 4.6	Strong	Weak/none	Yes	Strong	Yes
DZ 4.7	Weak	Weak/none	Yes	Strong	Yes
DZ 4.8	Weak	None	Yes	Strong	Yes
DZ 4.9	Weak	None	Yes	Strong	Yes
DZ 4.10	Strong	Strong	Yes	Strong	Yes
DZ 4.11	Weak	Weak	Yes	Strong	Yes
DZ 4.12	Strong	Strong	Yes	Strong	Yes
DZ 4.13	Strong	Weak	Yes	Strong	Yes
DZ 4.14	Strong	Weak	Yes	Strong	Yes

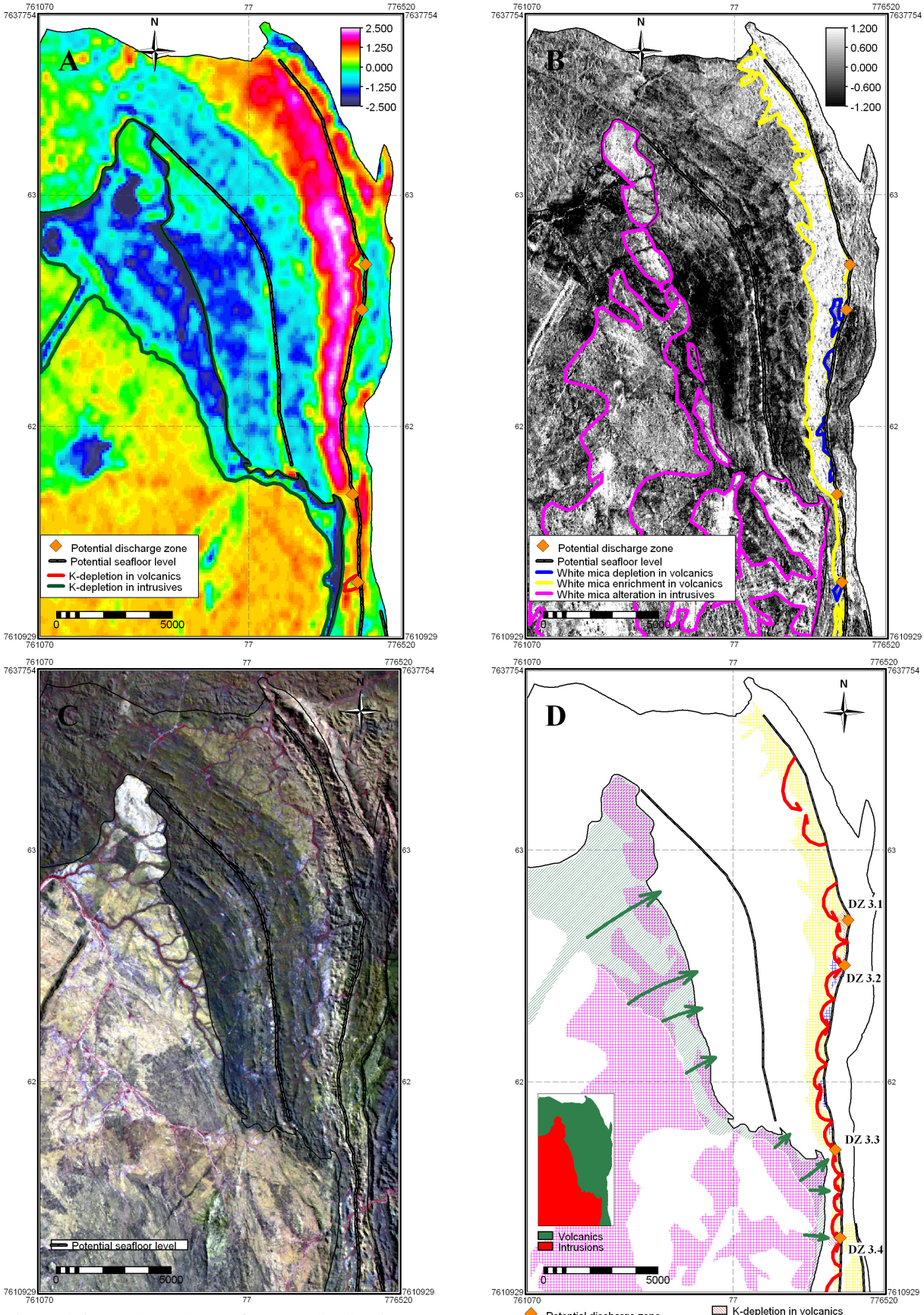

Figure 5.6: Northern Shaw: (**A**) normalised K-image; (**B**) normalised ratio image; (**C**) Landsat TM imagery false color composite; (**D**) hydrothermal alteration systems and lithology in inset.

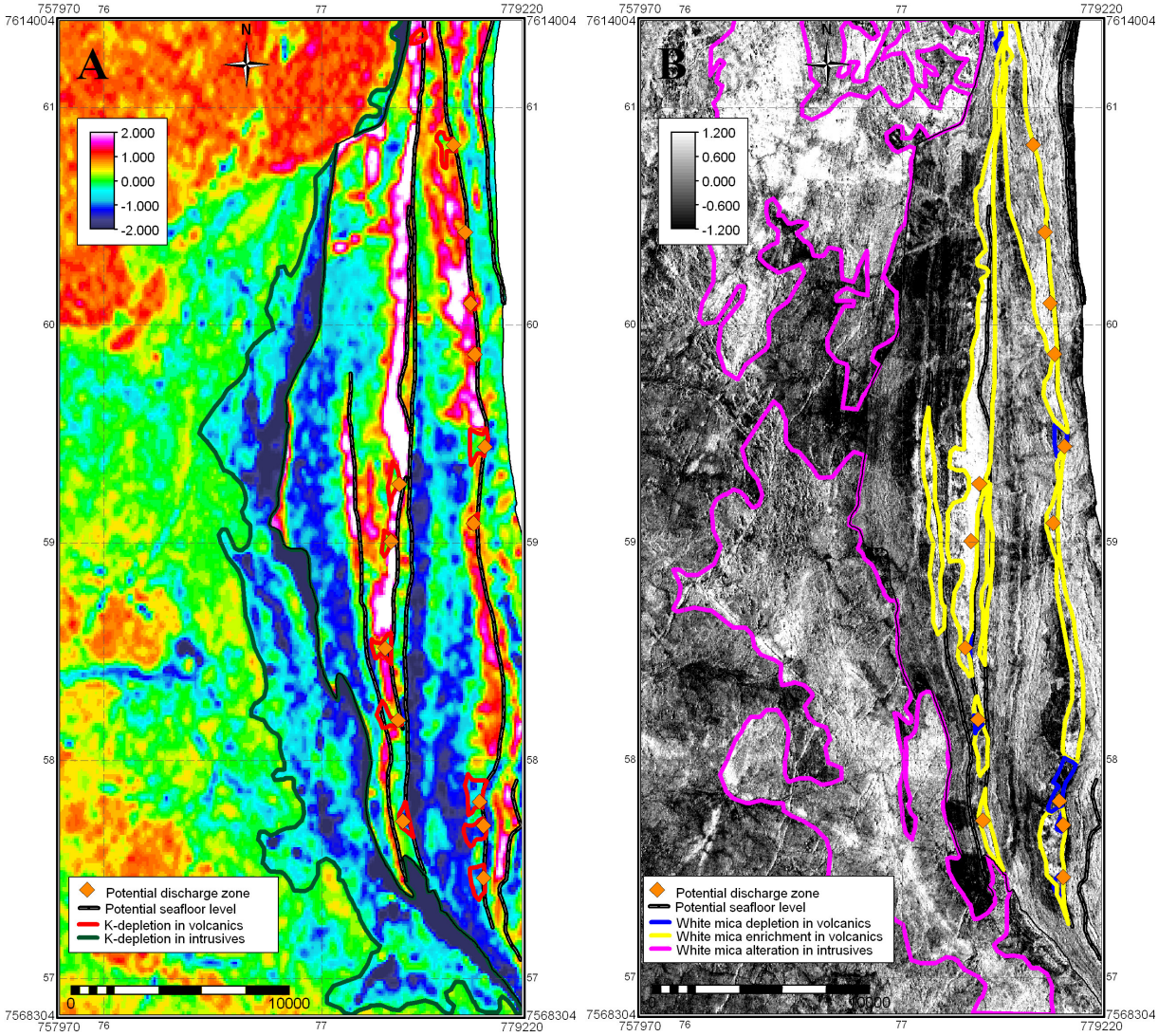

Figure 5.7: Eastern Shaw: (**A**) normalised K-image; (**B**) normalised ratio image; (**C**) Landsat TM imagery false color composite; (**D**) hydrothermal alteration systems and lithology in inset. [(C) and (D) are on next page.]

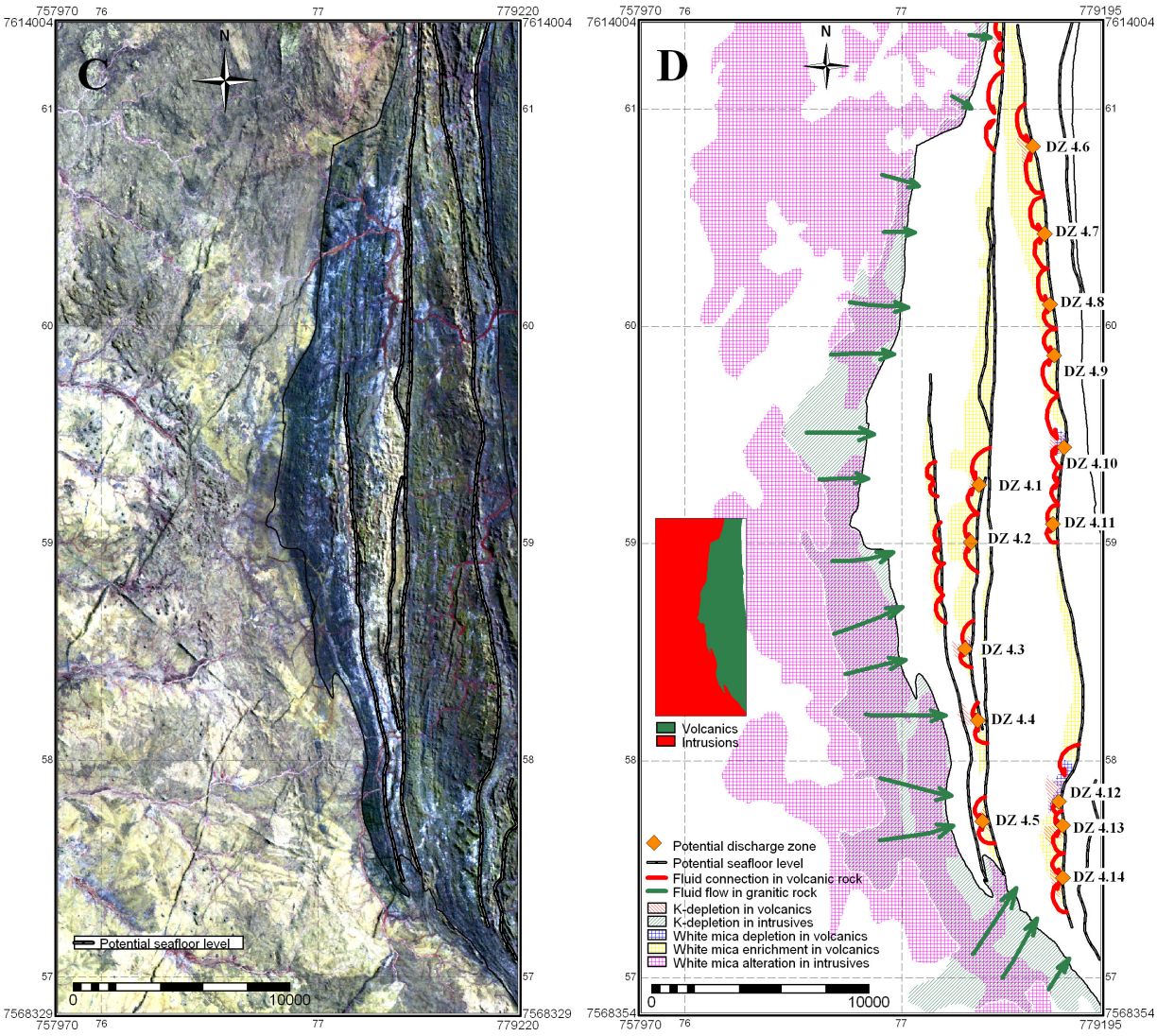

Figure 5.7: continued from previous page

CHAPTER 6: Discussion

In this chapter the research results are discussed. First, the map showing favourability for hydrothermal alteration systems that are related to VhMS deposit in EPGGT (Figure 6.1) is validated.

6.1. Validation of interpreted hydrothermal systems using known mineral deposits

Figure 6.1 shows hydrothermal alteration systems and potential discharge zones, which were interpreted in chapter 5, and known VhMS and other mineral deposits in EPGGT. Only in area 1 there are several known VhMS deposits. The two main deposits – Sulphur Springs (SS) and Kangaroo Caves (KC) – and four prospects – Breakers (BK), Man of War (MW), Anomaly 45 (45) and Roadmaster (RM) are evenly distributed [9] at top of the volcanic pile of Strelley in area 1. Existing SS, KC, MN and 45 deposits were almost in the same place with DZ 1.2, DZ 1.1, DZ 1.5, and DZ 1.6 respectively. Between BK and DZ 1.3 had about 500-600 meters difference. But considering the Brauhart alteration classes [3], BK occurs in a small chlorite-quartz alteration, which is not clear in the normalised images, as compared with bigger discharge zone next to it, which is DZ 1.3. DZ 1.7 is related with hydrothermal alteration system of RM prospect.

There is not any known VhMS deposit in areas 2 and 4. However, there are many precious metal (predominantly gold) deposits that have been classified as vein and hydrothermal-undivided mineralisation in those areas.

The relation between the precious metal deposits and the indications of hydrothermal alteration is not known and should be followed up in the field.

In area 3, there is only one known VhMS deposit named Sharks Gully 2 (Cu) in this area. But it is located in undefined greenstone - low magnetisation, which was classified by “rock” in the geological map that was not included for normalisation. Along the first paleo seafloor level (Figure 5.6 D), there are several precious metal deposits distributed.

6.2. Potential discharge zones

There are 38 potential discharge zones interpreted during in study. They are weighted based on the alteration rates (Table 6.1) where K depletion in volcanics has a high score (30), which is most important indicator of potential discharge zone, white mica depletion in volcanics has 15, white mica presence in recharge zone has 20, K depletion in intrusions has 20 and white mica alteration has 15. The final weight of a potential discharge zone is the sum weight of the scores of indications (max 100).

According to the Table 6.1, the average of being potential discharge zone in each area is over eighty, which means a high. Kangaroo Caves has 88 of favourability, which is known VhMS deposit. Therefore, 17 potential discharge zones can be very high favourability of being VhMS deposits that over 88 of favourability.

Generally, from the result of this study, most interpreted discharge zones are not associated with known VhMS deposits except area 1. There can be following reasons:

- Deposits have not been discovered yet;
- Wrong interpretation of remote sensing imagery;
- Known deposit is not classified as a VhMS deposit;
- Maybe conditions were not favourable for deposition of mineralisation;
- Alteration is related to shear zones.

In most cases, the methods of this study worked well and successful. For instance, detection of K depletion in discharge zones in volcanics from normalised gamma-ray images was simple and clear. Also white mica distributions related to recharge zones in volcanics and to alteration in intrusions, were detectable by the normalisation.

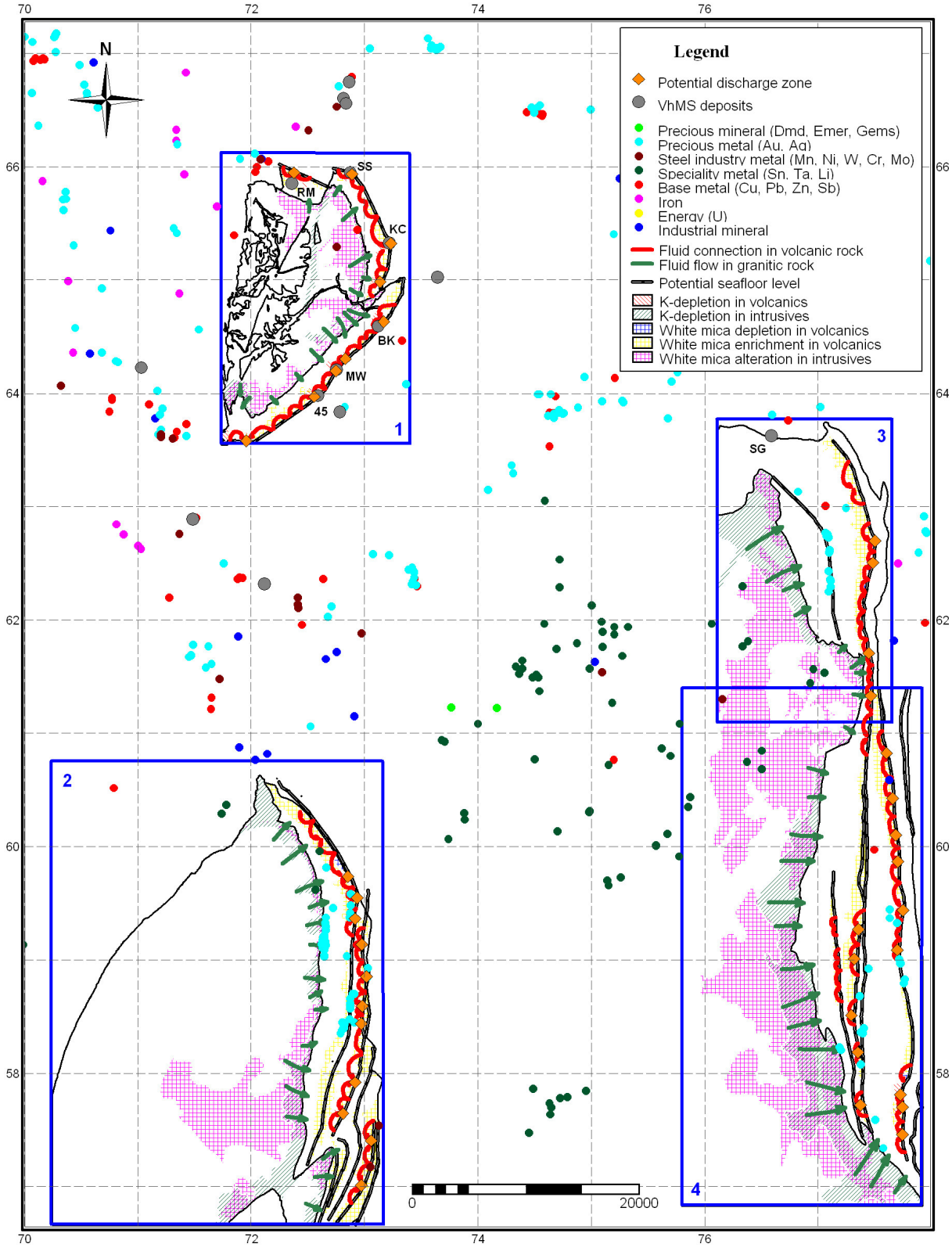

Figure 6.1: Interpreted hydrothermal alteration systems and mineral deposits in EPGGT (covering areas in chapter 5).

Table 6.1: Weights of potential discharge zones in EPGGT based on alteration rates.

Area 1		Area 2		Area 3		Area 4	
DZ 1.1	88	**DZ 2.1**	85	**DZ 3.1**	88	**DZ 4.1**	73
DZ 1.2	84	**DZ 2.2**	94	**DZ 3.2**	79	**DZ 4.2**	73
DZ 1.3	90	**DZ 2.3**	100	**DZ 3.3**	73	**DZ 4.3**	94
DZ 1.4	75	**DZ 2.4**	85	**DZ 3.4**	85	**DZ 4.4**	100
DZ 1.5	90	**DZ 2.5**	75			**DZ 4.5**	88
DZ 1.6	78	**DZ 2.6**	73			**DZ 4.6**	90
DZ 1.7	90	**DZ 2.7**	88			**DZ 4.7**	75
DZ 1.8	69	**DZ 2.8**	79			**DZ 4.8**	73
DZ 1.9	88	**DZ 2.9**	73			**DZ 4.9**	73
		DZ 2.10	85			**DZ 4.10**	100
		DZ 2.11	80			**DZ 4.11**	79
						DZ 4.12	100
						DZ 4.13	94
						DZ 4.14	94
Overall: 84		**Overall: 83**		**Overall: 81**		**Overall: 86**	

Also the geological settings in the 4 areas are probably not identical. This made it difficult to correctly interpret alteration systems and paleo seafloor level. Differences in study areas be due to:

- Variation in volcanic units between areas;
- Deformation;
- Metamorphic grade;
- Differences in thickness of volcanic sequences;
- Maybe geological process is not completely understood.

During the mapping process, the regional geology map was very important for calculation of average values of K and white mica distribution within the lithology units but the original regional geology map has some shifts that effected calculation and results. For instance, the boundary between volcanics and underlying intrusions in the middle part of the area 4 (Figure 5.7C), there were around 250-300 m boundary shifts to volcanics from intrusions. Therefore it was mapped as a high K concentration (Figure 5.7A), seemed there was maybe felsic volcanics. In reality, volcanics and intrusions, which were used in normalisation, were dominantly mafic and felsic rocks respectively. For that reason, interpretation of paleo seafloor level was complicated as well. Generally, study area covered very broad district and hydrothermal activity itself involves big region and regional hydrothermal systems within research area was detectable.

CHAPTER 7: Conclusions and Recommendations

This chapter has two sections; the first section focuses on research conclusions and the second section deals with recommendations for further research in the field of uncertainty.

7.1. Conclusions

Based on the work done, conclusions are as follows:

- Airborne imagery showing potassium concentrations that were normalised to lithology, can be used to indicate:
  - Felsic volcanic rocks in a volcanic sequence;
  - Potassic altered mafic volcanic rock related to recharge processes;
  - Crosscutting potassium depletion in felsic volcanics related to discharge processes
  - Potassium depletion due to hydrothermal alteration in and felsic intrusions related to discharge processes.
- Ratio (ATAN (band5 / band7) imagery of Landsat TM normalised to lithology, that potentially shows variation in white mica content can be used to indicate:
  - White mica altered volcanic rock, related to recharge related processes;
  - Possibly felsic metamorphosed rock;
  - Hydrothermal alteration in felsic (granitic) intrusions.
- Potential VHMS deposits are located in areas where crosscutting discharge related alteration intersects the paleo-seafloor at the top of a bi-modal volcanic sequence. Therefore detection of the top of a volcanic sequence that is felsic and the position of the paleo-seafloor has a high priority in detection of potentially mineralised areas.
- The EPGGT is the most prospective area for VhMS exploration and potential VhMS discharge zones are detected successfully by mapping variations in K concentration using regional gamma-ray spectrometry and the distribution of alteration minerals from Landsat TM.

7.2. Recommendations

Finding VhMS deposit is still an important issue for exploration geologists in EPGGT and there are few recommendations for future exploration at the end of this research study:

- The understanding of geological evolution and classification of lithological units in EPGGT is still somewhat in dispute and needs more study and mapping of geological setting.
- Other greenstone belts have to be studied as well. For instance the east-south part of the Corruna Down complex with volcanic sequence for VhMS exploration.
- The application of higher spectral and spatial resolution images to detect white mica discharges in potential discharge zone.
- Further field work for validation of potential discharge zones and mineralisation.

References

[1] Pirajno, F., Hydrothermal Mineral Deposits: Principles and Fundamental Concepts for the Exploration Geologists. 1992, Berlin Heidelberg New York London Paris Tokyo Hong Kong Barcelona Budapest: Springer-Verlag. 709.

[2] Spatial information for the Nation. 2003, Australian Government http://www.ga.gov.au/rural/projects/.

[3] Carl W. Brauhart, D.I.G., and Peter Morant, Regional Alteration Systems Associated with Volcanogenic Massive Sulfide Mineralization at Panorama, Pilbara, Western Australia. Economic Geology, 1998. 93: p. 292-302.

[4] C. W. Brauhart, D.L.H., D. I. Groves, E. J. Mikucki, and S. J. Cardoll, Geochemical mass-transfer patterns as indicators of the architecture of a complete volcanic-hosted massive sulfide hydrothermal alteration system, Panorama district, Western Australia. Economic Geology, 2001. 96: p. 1263-1278.

[5] Van Ruitenbeek, F.J.A., M. Hale, T. Cudahy, and F. van der Meer. Remote Detection Of Hydrothermal Fluid Paths By Spatial Analysis Of Gamma-Ray And Hyperspectral Imagery. in International Geochemical Exploration Symposium. 2003. Dublin, Ireland: Poster presentation.

[6] D. L. Huston, C.B., P. Wellman, and A. S. Andrew, Gamma-ray spectrometric and oxygen-isotope mapping of regional alteration halos in massive sulphide districts: an example from Panorama, central Pilbara Craton. AGSO Research Newsletter, 1998. 29.

[7] Scott, B.L.D.a.K.M., Interpretation of areal gamma-ray surveys-adding the geochemical factors. AGSO Journal of Australian Geology & Geophysics, 1997. 17(2): p. 187-200.

[8] M. J. van Kranendonk, A.H.H., R. H. Smithies, D. R. Nelson, and G. Pike, Geology and tectonic evolution of the archean north Pilbara terrain, Pilbara craton, Western Australia. Economic Geology, 2002. 97: p. 695-732.

[9] I.Ruddock, K.M.F.a., Mineral Occurrences and Exploration Potential of the East Pilbara. 2001, Department of Mineral and Petroleum Resources, GSWA: Perth.

[10] D. L. Huston, S.-S.S., R. Blewett, A. H. Hickman, M. Van Kranendonk, D. Phillips, D. Baker, and C. Brauhart, The Timing of Mineralization in the Archean North Pilbara Terrain, Western Australia. Economic Geology, 2002. 97: p. 733-755.

[11] Satellite Imagery, Landsat TM, http://www.agrecon.canberra.edu.au/Products/Satellite_Imagery/Landsat_TM/Landsat_TM.htm#.

[12] Geological Survey of Western Australia, http://www.agso.gov.au/.

[13] Van Kranendonk M.J., Geology of the North Shaw 1:100000 sheet. 2000: Geological Survey of Western Australia. p. 86.

[14] Common Remote Sensing Method Pool, http://www.geogr.uni-jena.de/~arsgisip/rs_pools/Methodpool/.

Appendix A: ILWIS Script for Normalisation

```
rem normalise image based on classified gis layer
rem syntax: normalise <image file> <classified raster map>
%1_%2crt.tbt = TableCross(%1.mpr,%2.mpr,%1_%2crt,IgnoreUndefs)
calc %1_%2crt.tbt
opentbl %1_%2crt.tbt
tabcalc %1_%2crt avg {vr=::0.000001}= aggavg(%1,%2,NPix)
tabcalc %1_%2crt stdev {vr=::0.000001}= aggstd(%1,%2,NPix)
tabcalc %1_%2crt norm {vr=::0.000001}= (%1-avg)/stdev
closetbl %1_%2crt.tbt
%1_%2avg.mpr{dom=VALUE.dom;vr=::0.000001}=MapAttribute(%1_%2crt,%1_%2crt.tbt.avg)
%1_%2stdev.mpr{dom=VALUE.dom;vr=::0.000001}=MapAttribute(%1_%2crt,%1_%2crt.tbt.stdev)
%1_%2norm.mpr{dom=VALUE.dom;vr=::0.000001}=MapAttribute(%1_%2crt,%1_%2crt.tbt.norm)
calc %1_%2avg.mpr
calc %1_%2stdev.mpr
calc %1_%2norm.mpr
```

Appendix B: Lithology description of regional geology map of EPGGT

Rock type	Description
Chemical sediment	Sediment; low, medium and high magnetization; jaspillite; chert; boulder conglomerate, sandstone, mudstone; carbonate rock; basalt, tuff etc.
Chemical sedimentary	Sediment; medium magnetisation
Classic sediment (Classic sedimentary)	Sediment; high magnetisation; ferruginous sandstone, siltstone, shale and chert; grit and sandstone with some conglomerate beds
Felsic extrusive	Rhyolite to dacite lava
Intermediate extrusive	Tuff
Mafic extrusive	Basalt; low, medium and high magnetisation; agglomerate, tuff and lava, chiefly dacitic; dolerite; basaltic andesite, and unsubdivide mafic volcanic rocks
Granite	Granite, flat, low, high and very high magnetisation; undifferentiated, unexposed granite; hornblende-adamellite/quartz-monzonite; massive and pillowed tholeiitic basalt, chert, tuff and felsic rocks
Felsic intrusive	Felsic porphyry; granite, medium magnetisation; pegmatite vein; hornblende porphyry dyke, related to –Pgh; quartz-plagioclase porphyry dyke; gabbro dyke or sill
Intermediate intrusive	Diorite; dark feldspar-quartz-biotite porphyry
Mafic intrusive	Gabbro & dolerite; low and high magnetisation; ultramafics, highly magnetic; pillowed and massive basalt, volcaniclastic rocks, shale, sandstone, chert, carbonate, conglomerate; gabbro dyke or sill
Gabbro	Gabbro (Gidley Granophyre); porphyritic, fine to medium grained granophyre (Gidley Granophyre)
Dolerite	Dolerite Dyke
Felsic rock	Felsic rock; low, medium and high magnetisation
Quartz	Quartz
Vein	Quartz
Ultramafite	Peridotite; ultramafic rock (not subdivided); concordant or subcordant peridotite, serpentinite or altered serpentinite; tremolite/actinolite +/- chlorite rock. Generally schistose; serpentinite; talc schist, mostly with chlorite, actinolite and carbonate; ultramafics, low and medium magnetisation
Metabasite	Amphibole-plagioclase schist
Greenstone	Low, medium and high magnetisation, mixed rocktypes (granite, gneiss & greenstone); boulder conglomerate, sandstone, mudstone, schistose psammitic, psammopelitic and pelitic metasediments, shale, siltstone, and arkosic sandstone, quartzite
Rock	Undefined greenstone; flat, low, medium and high magnetisation